Tectonophysics 608 (2013) 884–903

Contents lists available at ScienceDirect

Tectonophysics

journal homepage: www.elsevier.com/locate/tecto

Geodynamics of the Tavşanlı zone, western Turkey: Insights into subduction/obduction processes

Alexis Plunder [a,b,c,*], Philippe Agard [b,c,d], Christian Chopin [a], Aral I. Okay [e]

[a] Laboratoire de géologie, Ecole Normale Supérieure, UMR CNRS 8538, 24 rue Lhomond, 75005 Paris, France
[b] UPMC Univ. Paris 06, ISTEP F-75005, Paris, France
[c] CNRS, UMR 7193, F-75005, Paris, France
[d] IUF, F-75005 Paris, France
[e] Eurasia Institute of Earth Sciences and Department of Geology, Istanbul Technical University, Maslak, 34469 Istanbul, Turkey

ARTICLE INFO

Article history:
Received 24 May 2013
Received in revised form 18 July 2013
Accepted 21 July 2013
Available online 30 July 2013

Keywords:
Subduction
Obduction
Tavşanlı zone
Accretionary complex processes
PT estimates

ABSTRACT

The tectono-metamorphic evolution of the high-pressure low-temperature (HP–LT) Tavşanlı zone (Western Anatolia, İzmir–Ankara suture zone) is herein reappraised to highlight processes occurring along a fossil subduction interface, from initial obduction stages to continental subduction. Structural and petrological data allow in particular to constrain the nature, internal structure and PT conditions of the oceanic accretionary complex sandwiched between the subducted continental margin of the Anatolide–Tauride Block (Orhaneli unit) and the non-metamorphic obducted ophiolite on top. Two distinct oceanic units (termed complexes 1 and 2) are recognised on top of one another, with metamorphic conditions ranging from incipient HP-LT imprint (complex 1) to blueschist facies conditions (complex 2). Based on the first occurrence of Fe–Mg carpholite and on pseudosection calculations, PT estimates of 250–350 °C and 11–13 kbar are inferred for complex 2. The internal structure of the accretionary complex points to the underplating of kilometre-scale units at different depths along the plate interface and to contrasting dynamics with respect to both the underlying continental unit and the ophiolite. Inter-plate mechanical coupling within the Tavşanlı zone is compared to the Oman case-study. The variable HP–LT overprint of the metamorphic sole places further constraints on regional scale tectonics, the accretionary dynamics and on the rapid thermal reequilibration of the subduction interface.

1. Introduction

High-pressure low-temperature (HP–LT) rocks/terranes returned from subduction zones convey essential information on deep processes such as exhumation mechanisms (Ernst, 1973; Jolivet et al., 2003; Platt, 1993), long-term mechanical coupling (Agard et al., 2009; Angiboust et al., 2012a,b) or mass and fluid transfer (Marschall and Schumacher, 2012). They may either correspond to pieces of ocean-floor (Angiboust and Agard, 2010; Kienast, 1983), accreted sedimentary material (Agard et al., 2002; Cloos and Shreve, 1988a; Plunder et al., 2012) or rocks derived from continental crust (Chopin et al., 1991).

The İzmir–Ankara suture zone (İAZS; Fig. 1) is a major witness of the Mesozoic convergence between Gondwana-derived terranes (Anatolides, Taurides) and Eurasia. South of the İAZS, the predominantly continental-derived HP–LT Tavşanlı terrane underwent incipient blueschist to blueschist–eclogite facies conditions during the late Cretaceous (Çetinkaplan et al., 2008; Davis and Whitney, 2006, 2008; Okay, 1978, 1980a, 1980b, 1982, 2002; Okay and Kelley, 1994; Whitney and Davis, 2006) and is overlain by a fragment of unmetamorphosed oceanic lithosphere, the Anatolian ophiolite. The Tavşanlı zone is thus generally regarded as the (cover of the) northern continental passive margin of the Anatolide–Tauride Block dragged into subduction as a result of obduction (Gautier, 1984; Okay et al., 1998). Similar settings with obducted ophiolites atop HP–LT continental rocks are found in Oman (Bailey, 1981; Michard et al., 1981; Goffé et al., 1988), Zagros (Angiboust et al., 2013) or New Caledonia (Agard and Vitale-Brovarone, 2013; Black et al., 1993).

The Tavşanlı zone represents an ideal target to study obduction/subduction processes as (1) it represents an extensive HP–LT province (i.e., >Oman) beneath one of the world largest obducted ophiolites (since all Anatolian ophiolites derive from the same ocean; Okay and Whitney, 2010; Pourteau et al., 2010; Van Hinsbergen et al., 2010), (2) it is well-preserved, thanks to later mild collision, and (3) it corresponds to the onset of an unusually long-lived subduction of continental material to depth of 15–80 km (>30 My, from ~85–80 to 50–35 Ma). Subducted continental material comprises the Tavşanlı zone (which reached 50–80 km depth), the Afyon zone (15–45 km depth) and part of the Menderes Massif (15–45 km depth), hence ~450 km, from north to south, of subducted Anatolide–Tauride block (Fig. 1; Okay and Kelley, 1994; Okay et al., 1998; Sherlock et al., 1999; Seaton et al.,

* Corresponding author at: Laboratoire de géologie, Ecole Normale Supérieure, UMR CNRS 8538, 24 rue Lhomond, 75005, Paris, France. Tel.: +33 6 30 90 07 40.
E-mail address: plunder@geologie.ens.fr (A. Plunder).

0040-1951/$ – see front matter © 2013 Elsevier B.V. All rights reserved.
http://dx.doi.org/10.1016/j.tecto.2013.07.028

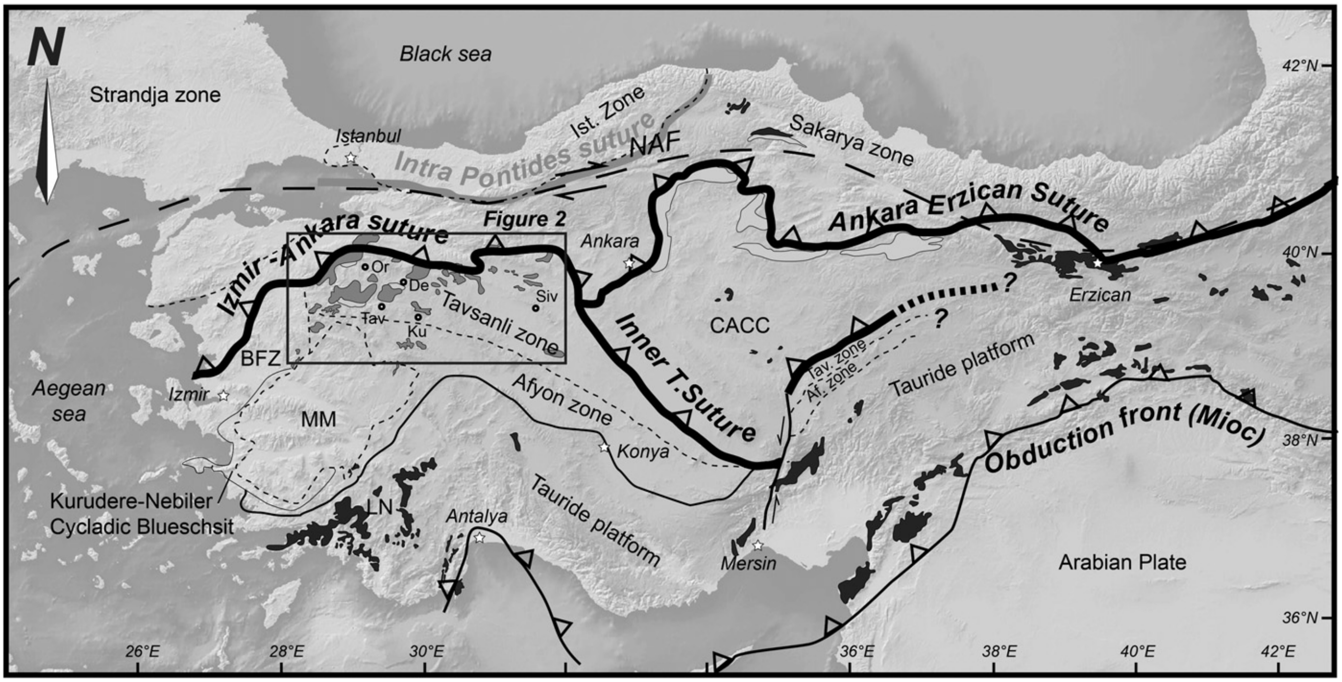

Fig. 1. Tectonic map of Turkey and surrounding areas showing the main suture zone. Black bodies refer to Anatolia ophiolite corresponding to the Izmir–Ankara–Erzican suture. Dark grey refers to ophiolitic bodies of the study area. Light grey bodies refer to cretaceous accretionary complex or so-called mélange. Geological units abbreviation are the following, BFZ: Bornova Flysh Zone; CACC: Central Anatolian Crystalline Complex; LN: Lycian Nappes; MM: Menderes Massif; NAF: North Anatolia Fault; Location names, De: Devlez; Ku: Kütahya; Or: Orhaneli; Siv: Sivrihisar; Tav: Tavşanlı. Modified after Jolivet et al., 2013; Moix et al., 2008; Okay and Tüysüz, 1999; Pourteau, 2011. Topography from Geomapapp 3.3.6 (http://www.geomapapp.org/).

2009; van Hinsbergen et al., 2010; van Hinsbergen and Schmid, 2012; Gessner et al., 2013; Pourteau et al., 2013).

Unfortunately, the deformation patterns, large-scale metamorphic trends and tectonic setting of the Tavşanlı zone remain poorly known. The present field-based contribution therefore attempts to (a) provide critical structural data, cross-sections, petrological observations and PT estimates on these extensive exposures of subduction interface rocks, (b) set back their evolution within the frame of regional geodynamics (i.e., convergence between Eurasia and Anatolides–Taurides), and (c) characterize mechanisms of burial, accretion and exhumation and compare them to the classical Oman case study.

2. Regional geodynamics

The Tavşanlı zone is found south of the Alpine İAZS (Fig. 1). This suture zone corresponds to the remnant of the major Neotethys ocean, which separated Laurasia and Gondwana from the mid-late Triassic (Tekin et al., 2002) to its closure during the late Cretaceous (in the west) or early Tertiary (in the east; Meijers et al., 2010; Lefebvre et al., 2013). It extends from north of İzmir to the border of Georgia, where it connects with the Sevan–Akera suture (Khain, 1975; Okay and Tüysüz, 1999). This suture is also connected farther to the west, across the Aegean domain, to the Vardar suture (Jolivet et al., 2013; Schmid et al., 2008).

The İAZS divides Western Anatolia in two major tectonic units, the Pontides and the Anatolides–Taurides platform (Okay et al., 1998; Sengör and Yılmaz, 1981). North of the suture zone, the Pontides comprise the Sakarya, İstanbul, and Rhodope–Strandja zones, which are part of Eurasia since the late Jurassic at least (Meijers et al., 2010; Moix et al., 2008). South of the İASZ, the Anatolide–Tauride Block shows stratigraphic similarity with the Arabian platform and a Pan-African basement (dated at 541 ± 14 and 566 ± 9 Ma using U/Pb on zircon; Gessner et al., 2004), which advocate for a Gondwanian origin (Okay and Tüysüz, 1999; Sengör and Yılmaz, 1981). Readers are referred to Sengör and Yılmaz (1981), Okay and Tüysüz (1999), Moix et al. (2008) and reference cited herein for further information about the palaeogeography of Turkey.

Along a 300 km portion (Fig. 1), the Sakarya zone is in contact with the regional blueschist belt of the Tavşanlı zone. The Tavşanlı zone represents the northernmost extension of the Anatolide–Tauride Block passive margin (Okay et al., 1998) subducted below some oceanic lithosphere during the late Cretaceous. Western Anatolia indeed shows widespread high-pressure–low-temperature rocks and obducted ophiolites (Candan et al., 2005; Collins and Robertson, 1997; Davis and Whitney, 2006, 2008; Dilek et al., 1999; Droop et al., 2005; Gautier, 1984; Monod et al., 1991; Okay, 1978, 1980a,b; Okay and Kelley, 1994; Okay and Tüysüz, 1999; Parlak and Delaloye, 1999; Rimmelé et al., 2004; Robertson, 2002; Whitney and Davis, 2006). The regional setting is very similar to the one observed in Oman (Goffé et al., 1988; Searle et al., 1994), with intra-oceanic subduction preceding obduction, which starts at *ca.* 95 Ma and continental subduction at ~80 Ma, or in New Caledonia (Black et al., 1993). A detailed description of the Tavşanlı zone is given in the next section. After the disappearance of all oceanic domains between Eurasia and the Anatolide–Tauride Block, the Tavşanlı zone underwent only mild collision (i.e., with comparison to the Himalayas: well-preserved, extensive HP–LT metamorphism near the suture zone, absence of widespread MP–MT metamorphism, lack of anatectic crustal melts, minor crustal thickening…). This may be related to the lack of subduction under Eurasia/Sakarya to the north and/or to its migration southwards through time, as observed in the Cyclades (Jolivet and Brun, 2008; Jolivet et al., 2013; Van Hinsbergen et al., 2010).

Western Anatolia hosts a wealth of high-pressure metamorphic terranes and ophiolitic bodies. The Afyon zone, which is thought to represent the southward palaeogeographic extension of the Tavşanlı zone (Candan et al., 2005), records HP metamorphism at *ca.* 65 Ma (Pourteau et al., 2010, 2013). HP metamorphism was also documented at *ca.* 45 Ma in the Kurudere–Nebiler unit located on the northern edge of the Menderes massif (Pourteau et al., 2013), which represents a likely eastern extension of the Aegean Pindos basin. Most ophiolites show

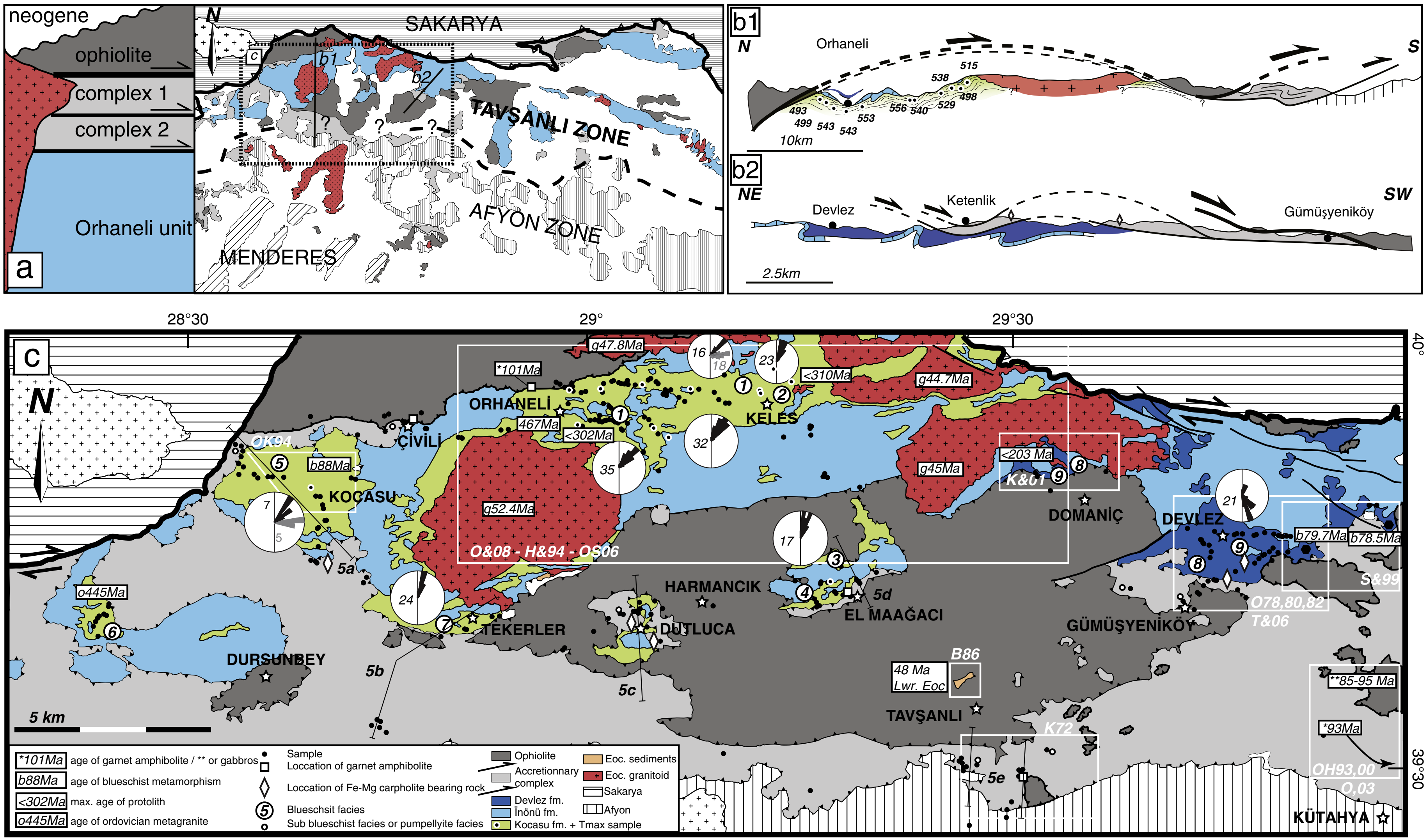

Fig. 2. (a) Simplified stratigraphic log of the Tavşanlı zone and simplified geological map of the Western part of Tavşanlı and Afyon zones (Modified from MTA, 2002). (b) Cross sections of the Orhaneli and Devlez region. (c) Simplified structural sketches of the study area, with location of detailed cross sections and sites selected for tectonic measurement (Lineation plotted). Number refer to high-pressure paragenesis, (1) gln + jd + phg + cld + lws (2) cld + jd (3) jd + lws (4) jd (5) gln + cld or jd + cld (6) gln + lws or cld + jd (7) gln + jd (8) gln + lws ± Na-Px (9) grt + lws + gln + phg ± Na-Px. Abbreviation after Kretz, 1983 ecxept for phg: phengite; Na-Px: Sodic pyroxene. White squares represent the study area of work mentioned in text, K72: Kaya, 1972; L72: Lisenbee, 1972; O78,80,82: Okay, 1978, 1980a,b, 1982; B86: Baş, 1986; OH93,00: Önen and Hall, 1993, 2000; H94: Harris et al., 1994; OK94: Okay and Kelley, 1994; S&99: Sherlock et al., 1999; O03: Önen, 2003; OS06: Okay and Satır, 2006; T&06: Topuz et al., 2006; O&08: Okay et al., 2008. Modified from MTA, 2002.

strikingly similar emplacement ages throughout Anatolia, sub-ophiolitic metamorphic rocks being dated from 95 to 90 Ma (Çelik et al., 2006; Dilek et al., 1999; Parlak and Delaloye, 1999). Some recent work by Çelik et al. (2011), however, documented ~170 Ma sub-ophiolitic metamorphic rocks along the İASZ north of Ankara, thus yielding the same metamorphic age as the Hellenide–Dinaridic ophiolite (Pamic et al., 2002). This could suggest that the İzmir–Ankara ocean was already subducting during the early-middle Jurassic (Topuz et al., 2012).

Several major geodynamic uncertainties nevertheless remain, as (i) the number of subduction zones in the Neotethys north of the Anatolide–Tauride Block during the Cretaceous. Jurassic metamorphic soles may support the existence of a subduction in the İzmir–Ankara ocean (Çelik et al., 2011), In the absence of clear evidence for subduction beneath Sakarya (Okay et al., 2001) or for any subduction zone south of the Tavşanlı zone (Shin et al., 2013) only one northward dipping intra-oceanic subduction is assumed in this study; (ii) similarly, the start of subduction across this region is poorly documented and the only certain (intra-oceanic) subduction event took place from *ca.* 95 Ma onwards; (iii) the triggering of this intra-oceanic subduction (i.e., as a result of the plate acceleration documented during the late Cretaceous?; Agard et al., 2007); (iv) the origin of the Western Anatolian ophiolitic nappes; they will herein be considered as unique, rooted in the İzmir–Ankara Suture, whose southern exposure (i.e., the Lycian nappes ophiolites; Fig. 1) are the result from post-convergence doming and extension (van Hinsbergen et al., 2010).

3. Geological setting of the Tavşanli Zone

This section reviews available data on the Tavşanlı zone. The Tavşanlı zone is an east–west trending, approximately 250–300 km long and >50 km wide high-pressure, continental derived belt. Three main units can be described (Okay et al., 1998), from bottom to top: (i) the Orhaneli blueschist sequence (northern continental margin of the Anatolide–Tauride block, formally the Tavşanlı zone); (ii) a Cretaceous accretionary or mélange complex (derived from the Tethyan ocean); (iii) an ophiolitic thrust sheet obducted over the continental margin.

3.1. Continental-derived units: the Orhaneli sequence

This unit is itself made up of three formations making a coherent stratigraphic series and mostly made up of metasedimentary rocks (Okay, 1986). At the bottom one finds the Kocasu formation (Okay, 2002; Okay and Kelley, 1994; Okay and Whitney, 2010), which consists of quartz-rich greyschists at the base and white phengite-rich schists at the top (Lisenbee, 1972; Fig. 3a,b). The thickness of the Kocasu formation is assumed to be >1 km (Okay, 2002; Okay and Kelley, 1994; Okay and Whitney, 2010). The age of this formation is poorly constrained by Ordovician and Permo-Carboniferous clastic zircons that give a post Carboniferous depositional age (Okay et al., 2008; Özbey et al., 2013a, 2013b). The basement of this formation was neither found in the Kocasu area (Fig. 2) nor in the Orhaneli region. An Ordovician metagranite was found in the region of Dursunbey and described as the basement of Orhaneli sequence (Özbey et al., 2013a). The greyschist formation shows a well-defined penetrative and gently dipping foliation (Lisenbee, 1972). Lineation is marked by mineral alignment of jadeite or chloritoid and occasionally sodic amphibole. Jadeite–glaucophane and chloritoid–glaucophane rocks were found in the western part of the Kocasu formation (Okay and Kelley, 1994). More unusual HP–LT assemblages (jadeite–chloritoid–glaucophane–lawsonite–phengite) were found in the Orhaneli region. Greyschists of the Kocasu formation give peak pressure–temperature estimates of 430 ± 30 °C–22 ± 4 k bar (Okay, 2002; Okay and Kelley, 1994), which yields an unusually cold geotherm of 5 °C/km for continental crustal rocks (Okay, 2002; Okay and Kelley, 1994). The age of metamorphism is poorly constrained, with radiometric ages ranging from 70 to 123 Ma (Ar–Ar on phengite; Okay and Kelley, 1994; Okay et al., 1998; Sherlock et al., 1999). The large spread of ages was attributed to excess argon during HP–LT metamorphism (Sherlock and Kelley, 2002; Sherlock et al., 1999). The age of peak metamorphic conditions in the Orhaneli unit is nevertheless commonly regarded as 80 ± 5 Ma (Ar–Ar on phengite; Sherlock et al., 1999).

The İnönü Marble (Servais, 1981) overlies the greyschists and shows a gradual facies evolution upwards (Lisenbee, 1972). This marble unit, which lacks a known substratum in the İnönü region, indeed gradually changes upward from massive marbles to intercalated quartzitic and phengitic marble layers and to an alternation of metagreywackes and metabasites (Servais, 1981, 1982). The latter section is equivalent to the Devlez formation described further west (Okay, 1980a, 1980b), where no progressive transition was observed. In the Devlez and Orhaneli regions (Fig. 2), the İnönü Marble is made of massive, banded white and grey marbles and consists of calcite replacing HP–LT aragonite (Okay and Whitney, 2010). The age of this 1 to 3 km thick formation is constrained by its resemblance to the Mesozoic Tauride platform series (Gutnic et al., 1979), which is further supported by the finding of upper Norian conodonts in the lower part of the marbles north–west of Domaniç (Kaya et al., 2001; Fig. 2). The İnönü formation is thought to extend to the lower Cretaceous on the basis of the regional ages of carbonate rocks (Gutnic et al., 1979). The few lineation measurements made so far on this unit strike N090 (Lisenbee, 1972) for the Orhaneli area.

On top of the marbles, a 5 to 10 m thick calcschist layer was observed at the base of the Devlez formation (Okay, 1980a, 1980b). The Devlez formation comprises metabasites, metacherts and metashales metamorphosed under blueschist conditions (Van der Kaaden, 1966; Lünel, 1967; Okay, 1980a, 1980b; Fig. 3d,e). Its thickness is <1 km (Okay, 1980a). The metabasite comprise glaucophane + lawsonite with the additional presence of sodic pyroxene, chlorite, titanite (Cogulu, 1967; Okay, 1980a, 1980b). Prograde metabasites can also be found in the lawsonite zone of Okay (1980a), with the assemblage sodic pyroxene + lawsonite + chlorite + quartz. Garnet is rare and spessartine-rich in the metacherts and the common assemblage is quartz + phengite ± sodic amphiboles ± garnet ± lawsonite ± hematite ± sodic pyroxene (Okay, 1980b). Metamorphic foliation is well-defined within the metachert and metashale, and stretching lineation is defined in places by sodic amphiboles. Despite former petrological studies the PT conditions of the Devlez formation are still poorly known. The only available peak PT data range between 300–500 °C and 8–12 kbar for epidote blueschists from the distant Konya region, which are thought to be equivalent to the ones in Devlez (Droop et al., 2005). Metamorphism was dated between 86 and 123 Ma using the Ar–Ar method on phengite (Sherlock et al., 1999). Those ages were probably overestimated due to excess argon, as phengite gave Rb–Sr ages of 78.5 ± 1.6 and 79.7 ± 1.6 Ma (Sherlock et al., 1999). Metamorphic ages for the blueschists of Sivrihisar region are consistent with those for the Orhaneli and Devlez areas and yield values between 80.1 ± 1.6 and 82.8 ± 1.7 (Rb–Sr on phengite) and 87.9 ± 0.3 Ma (Ar–Ar on phengite; Sherlock et al., 1999; Seaton et al., 2009).

3.2. The Cretaceous accretionary complex

The Cretaceous accretionary complex tectonically overlies the blueschist sequence. It has been first described by Kaya (1972) south of Tavşanlı (Ovacık complex) and by Lisenbee (1972) in the Orhaneli region. Although it was called 'ophiolitic melange' by these authors, it clearly lacks a matrix (whether shaly or serpentine-rich) that usually defines sub-ophiolitic mélange-type rocks (Festa et al., 2012). Lithological successions comprise mafic volcanic rocks, radiolarian cherts, green and red shale, and pelagic limestone (Kaya, 1972; Okay, 1982). Foliation is present along major fault zones were serpentinites occur (Okay, 1982). The thickness of this unit is highly variable and ranges between a few metres to ~1 km. The Ovacık complex was always found with the same tectonic setting (on top of the Orhaneli sequence or equivalent). This Cretaceous

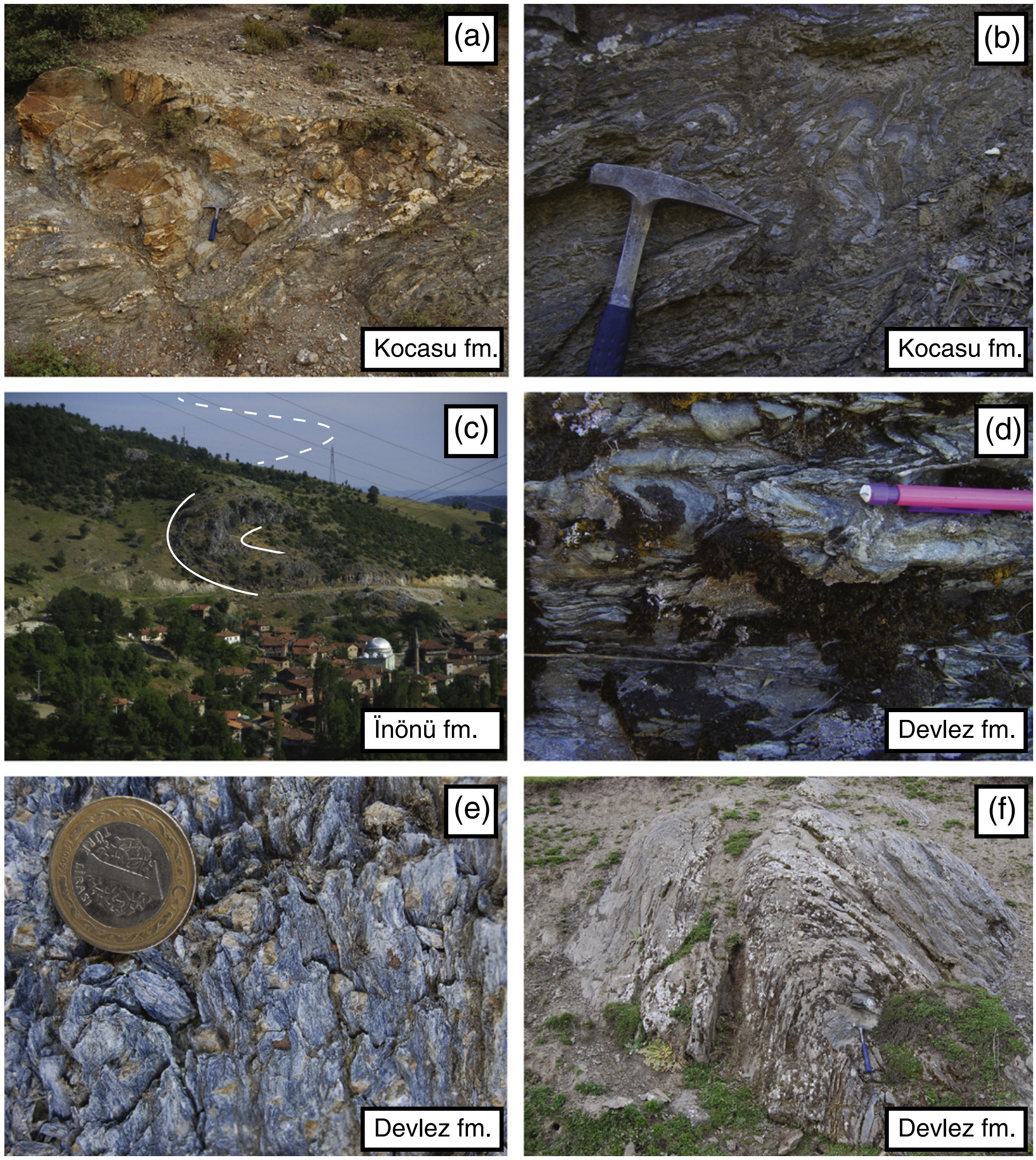

Fig. 3. Field photographs of: (a) Heart shaped sheath fold in the greyschists of Orahneli region; (b) Common small-scale folds in the greyschsits of Orhaneli region. (c) hm-scale fold in the İnönü formation of the Orhaneli region; (d) Small-scale fold axis in the quartzite of the Devlez formation, near Devlez locality; (e) Typical lws–gln bearing metabasite of the Devlez area; (f) Devlez fold, orientation of fold axis is N130.

accretionary complex was described all along the İzmir–Ankara suture zone, below the main ophiolitic body (Figs. 1,2a,b). Basalts are the most studied rocks of this accretionary complex and show various affinities including island oceanic tholeitic basalts and mid-ocean ridge basalts (Göncüoglu et al., 2006, 2010). Ages from radiolaria found in the cherts related to this accretionary complex range between the late Triassic and the late Cretaceous (Bragin and Tekin, 1996; Göncüoglu et al., 2006; Okay et al., 2012; Servais, 1981; Tekin and Göncüoglu, 2007, 2009; Tekin et al., 2002). Although metamorphism is not apparent in the field, except for spilitised basalts, high-pressure minerals are present at the thin-section scale (sodic pyroxene, lawsonite, aragonite; Okay, 1982). Aragonite has also been found as a prograde relic replacing primary micrite in pelagic limestones (Topuz et al., 2006). This demonstrates the HP–LT metamorphic imprint in the accretionary complex. Even though PT conditions are given to be different in the accretionary complex, most PT estimates indicates temperature under 200 °C and pressure values between 4 and 8 kbar (Okay, 1982; Topuz et al., 2006), based on the pumpellyite–actinolite and blueschist facies of Evans (1990) for the lower and upper PT conditions respectively. Occurrences of true, amphibole-bearing blueschists are described, but remain rare (Okay and Whitney, 2010). Metamorphism was not dated in this unit. It should have occurred between the Cretaceous and the Ypresian, as neritic limestones of the latter age are found overlying unconformably the accretionary complex (Özgen-Erdem et al., 2007; Servais, 1981).

3.3. The obducted ophiolite and associated metamorphic sole

An unmetamorphosed ophiolitic body rests tectonically atop the accretionary complex or the Orhaneli group. It is made of 90% partly serpentinized harzburgite and dunite, and 10% pyroxenites, chromitites, diabase dykes and rare gabbros (Lisenbee, 1972; Önen, 2003). This peridotite thrust sheet crops out as numerous klippen. The size of this ophiolitic klippe can be estimated to have been more than 250 km long and 100 km large, which makes it one of the largest obducted ophiolite worldwide. The Burhan ophiolite, north of Orhaneli was the subject of a detailed study (Lisenbee, 1972). Its thickness is estimated to 13 km, and the typical mineral assemblage of the peridotite is olivine + orthopyroxene + clinopyroxene + chromian spinel (Lisenbee, 1972; Önen, 2003; Önen and Hall, 1993, 2000). The peridotite has a supra-subduction zone signature and likely formed in a forearc context (Manav et al., 2004; Önen, 2003; Sarıfakıoğlu et al., 2009, 2010). At the base of the ophiolite, amphibolite-facies metamorphic sole rocks are found in places (Gautier, 1984; Monod et al., 1991; Okay et al., 1998; Önen, 2003; Önen and Hall, 1993). These metamorphic soles likely formed during the initiation of intra-oceanic subduction (Spray, 1984; Wakabayashi and Dilek, 2003; Woodcock and Robertson, 1977) as cold oceanic crust was brought in contact with the hot mantle. Assemblages consist of hornblende + plagioclase + epidote + quartz + rutile ± garnet and PT estimates give peak conditions of 8.5 ± 3.5 kbar and 700 °C (Okay et al., 1998; Önen and Hall, 2000). A high-pressure low-temperature overprint was observed, with the development of sodic amphiboles and fine lawsonite aggregates that give PT conditions of about 300 °C and at least 5 kbar (Okay et al., 1998; Önen and Hall, 2000). Similar observation was made in metamorphic soles of Sivrihisar area and southern Turkey (Dilek and Whitney, 1997; Gautier, 1984). Amphibolite metamorphism was dated using Ar–Ar cooling age on hornblende (Okay et al., 1998; Önen, 2003; Önen and Hall, 2000). Ages range between 93 and 101 Ma for metamorphic sole rocks of the Tavşanlı zone.

4. Structural data and key sections across the Tavşanlı zone

This paragraph reports tectonic (and petrological) observations made on several sections (located on Figs. 2a,c) across the Tavşanlı zone.

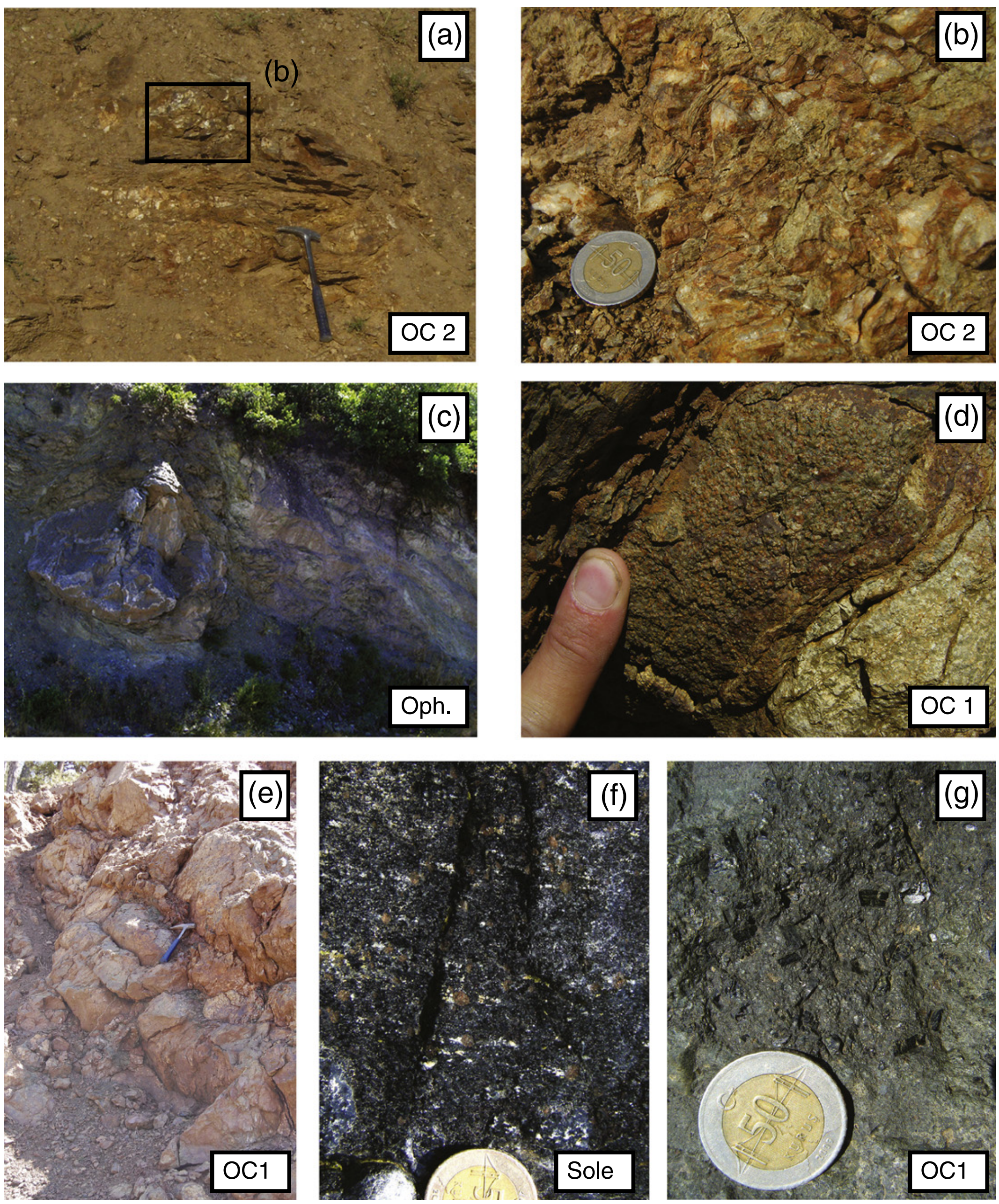

Fig. 4. Field photographs of: (a) Outcrop overview of a Fe–Mg Carpholite-bearing rock in the OC2, south of Kocasu cross-section; (b) zoom of (a), with green Fe–Mg carpholite fibbers; (c) Local true mélange at the basis of ophiolite, with pelagic limestone block in a tuff and serpentinite weak matrix, south of Tavşanlı; (d) Pillow basalt and associated variolites in OC1 south of Tavşanlı; (e) Well preserved pillow basalt with incipient metamorphism is OC1, near Gümüşyeniköy; (f) Metamorphic amphibolitic sole in the region of Çivili; (g) Preserved magmatic clinopyroxene in massive lavas of the OC1, north of Kocasu cross section.

4.1. Orhaneli region

In the area west of Orhaneli the greyschists show a horizontal to gently dipping foliation (Fig. 2b). Numerous folds were found at different scales, from few centimetres to tens of metres (Fig. 3a,b). Many folds consist of carbonated or siliceous elongated bodies deformed within a weaker schistose matrix. Fold axes were systematically measured in the Orhaneli region and the orientation is mostly NNW–SSE to NW–SE or E–W. There is no systematic relationship between the size, the nature of material and the trends of fold axes. Deformation in the marbles

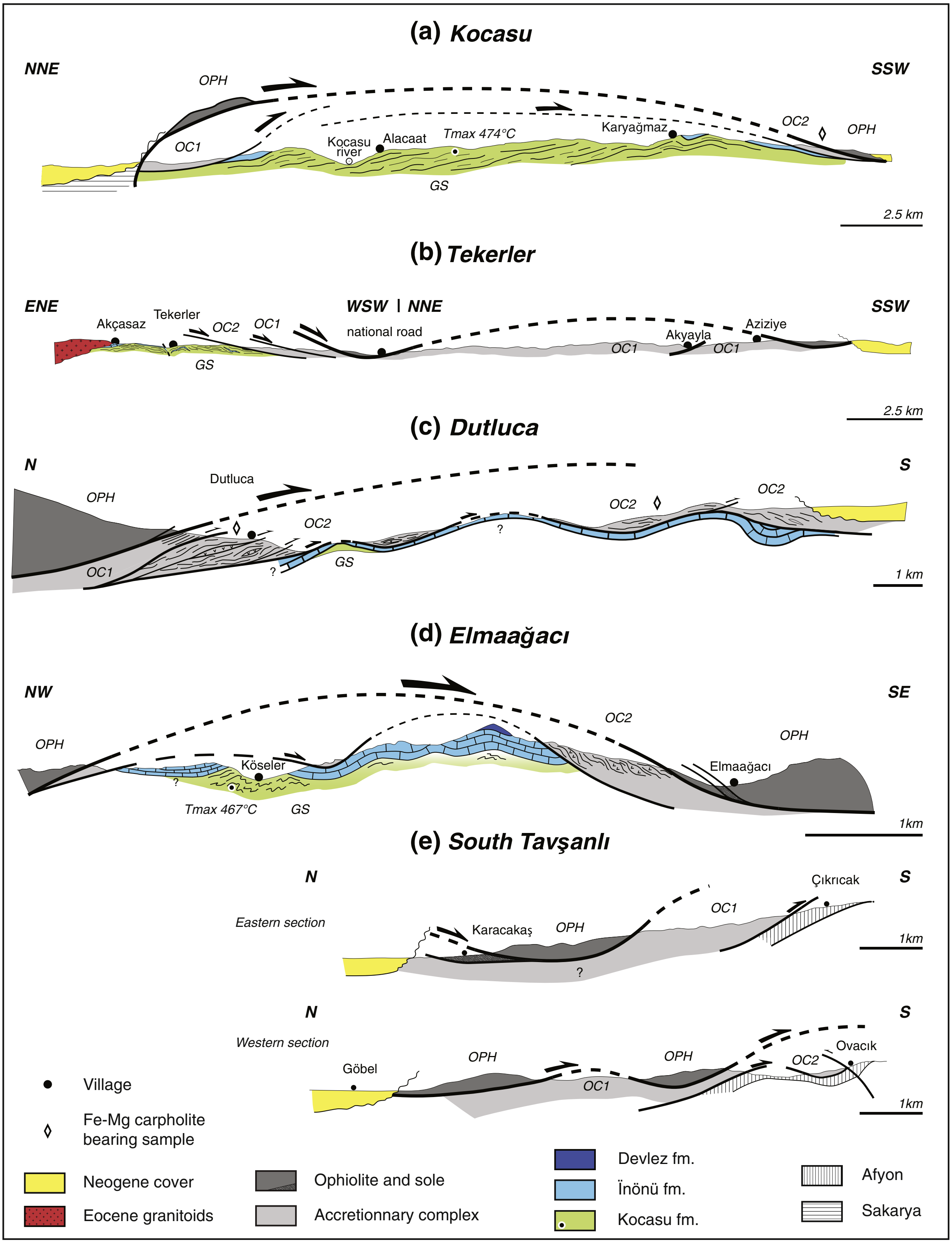

Fig. 5. Key cross section of the study area. Details are given in text.

consists of large tight to isoclinal folds, with hm- to km-scale wavelengths (e.g., near the village of Dedeler; Fig. 3c). Thickness variations are also conspicuous, as shown on Fig. 2b. The dominant stretching lineation, defined by minerals such as jadeite, chloritoid, lawsonite or phengite, strikes N020 to N040 (Fig. 2c). Unoriented glaucophane crystals are frequently found on the schistosity plane, which suggests later exhumation-related crystallisation post-dating the dominant phase of stretching. A late, dominantly N140–N155 trending stretching lineation was observed in places (and at N090 in one place). Previous work documented E–W trending lineations based on the elongation of calcite grains in the marble (Lisenbee, 1972). The Devlez formation was not found in this area, and the accretionary complex only crops out as a minor tectonic slice showing massive lavas, radiolarian cherts and metatuffs. The southern part of the cross section will be discussed in detail in the Tekerler section.

4.2. Kocasu region

The Orhaneli unit presents here some lithological differences with the one described farther to the east. At the top of the sequence, no transitional facies to the marbles is observed. Instead many intercalations of more basic material were observed, as described by Okay and Kelley (1994). The sequences down section mostly comprise quartzitic and felsic massive rocks. The foliation trend reveals a dome structure, with smaller folding at the scale of the outcrop (Fig. 5a). The Kocasu section shows minimal deformation in comparison with the Orhaneli area, and only one site was selected for tectonic measurements. The (NW–SE) trend of fold axes is similar to the one observed in the Orhaneli region. Stretching lineations, measured on a scale of approximately ten kilometres, evidence two clusters at N40 and N85 (Fig. 2c). The İnönü formation shows considerable variations in thickness, with only a thin level of marbles at each extremity of the cross-section. The Cretaceous accretionary complex thus directly overthrusts the greyschists in places (Fig. 5a). As seen in the cross-section (Fig. 5a) two types of accretionary complexes were distinguished. To the south, the existence of a high-pressure low-temperature metamorphic accretionary complex is attested by the presence of blueschist facies assemblages and impure quartzite bearing Fe–Mg carpholite (Fig. 4a,b). By contrast, a non-metamorphic or only slightly metamorphosed (Fig. 4g) succession of basalts, pillow breccia, and radiolarian cherts is found to the north. The latter complex was also found north of Çivili and west of Orhaneli granodiorite (Fig. 2c). Those accretionary complexes will be referred to hereafter as oceanic complex 1 (OC1) and 2 (OC2) according to their low and higher metamorphic grade, respectively. Northwest of this cross section, near the village of Çivili, hm-scale outcrops of garnet amphibolite (Figs. 2c,4f) are found at the base of the main Burhan ophiolite.

4.3. Tekerler region

Greyschist and marbles are found south of the Orhaneli granodiorite (Fig. 5b), where they are cut, in the vicinity of the main granitic body, by numerous dykes. Foliation dips to the south in the greyschists and fold axes strike dominantly W–E, with rarer NW–SE trending fold axes. Stretching lineations range between N015 and N020. To the south, the accretionary complex is again twofold, with (1) an OC2-type consisting of blue glaucophane and lawsonite bearing metatuffs and volcanic rocks lacking pervasive ductile deformation and (2) about one kilometre southward, a unit with similar lithologies but with a weaker metamorphic grade. This unit, referred to as OC1, is made of red radiolarian cherts, and green basaltic rocks. It is overthrust by a two kilometre wide peridotite klippe (Fig. 5b). South of the ophiolite klippe, OC1 shows a tectonic imbrication, with two distinct slices separated by a m-thick serpentinite sliver. OC1 lithologies are slightly different in this area, with one slice made of pillow basalts and massive lavas flows, and the other consisting of metatuffs and alternating cherts, pelagic limestones and basalts. To the south, the ophiolitic body is unconformably overlain by Neogene sediments near the village of Aziziye (Fig. 5b).

4.4. Dutluca

In the Dutluca region (west of Harmancık) the peridotite overthrusts both OC1 and OC2 with north-to-south senses of shear (Fig. 5c). OC1 consists of pyroclastic flows, pillow breccias, tuffs and radiolarian cherts and is locally very thin (~100 m). OC2 is thicker, showing numerous internal thrusts (e.g., between Dutluca and the Tavşanlı Dursunbey road). Those tectonic contacts are marked in the field by metric (to decametric) serpentinite slivers separating several hm-scale tectonic slices of oceanic complex. Pervasive ductile deformation is generally absent in OC2. It is made of metatuffs, basaltic lavas or pillows, Fe–Mg carpholite-bearing impure quartzites and radiolarian cherts. Most rocks show a clear blueschist-facies metamorphism, with the development of glaucophane and lawsonite $\pm$ a sodic pyroxene. The İnönü marble formation underneath is folded at the km-scale, shows large thickness variations and may be very thin or absent, as indicated by the presence of lawsonite–jadeite-bearing greyschists (Fig. 5c). To the south, relicts of OC2 are present on top of the marbles to the south, as attested by the presence of blueschist-facies rocks including Fe–Mg carpholite rocks (Figs. 2c,5c).

4.5. Elmaağacı

In the Village of Köseler (north of the section, Fig. 5d) greyschists show a N015 stretching lineations and major fold axes around NW–SE, as for most other greyschists occurrences (i.e. the Orhaneli, Kocasu and Tekerler regions). No gradual transition or tectonic contact was observed between the greyschists and the surrounding marbles. The thickness of the marble formation overlying the greyschists is <100 m to the south (Fig. 5d) but difficult to assess to the north. Marbles are overlain by cherts or mafic blueschists corresponding to the Devlez formation, without conspicuous deformation at the contact. A N010 stretching lineation is clearly visible in the cherts. One klippe of accretionary complex, comprising tuffs, rare mafic boudins and cherts is found on top of the marbles south of the main hill (Fig. 5d). The presence of glaucophane and lawsonite suggests that this unit is related to high-pressure OC2 found elsewhere. No Fe–Mg carpholite was found, however. At the serpentinized base of the main ophiolitic body, near the village of Elmaağacı a slice of amphibolite-facies metamorphic sole, described in greater detail in the next paragraph, is duplexed into the major contact (Fig. 5d). Note that the greyschists were not found in this part of the section. A parallel cross-section a few kilometres to the west (Fig. 2c) shows the same features, but it lacks the amphibolitic sole in the main ophiolitic contact and shows a more developed blueschist-facies sequence on top of the marbles.

4.6. South of Tavşanlı

Two parallel cross-sections were made south of Tavşanlı (Fig. 5e). The western section shows a chaotic, km-long unit with different rock types embedded in a serpentinite and tuffaceous matrix (Fig. 4c): (1) rocks typical of the accretionary complex (i.e., tuffs, radiolarian cherts, limestones, basalts and gabbros) and (2) fragments of serpentinite, silicified peridotite, peridotite and gneiss. A unit with basaltic flows, alternating tuffs and radiolarian cherts, and the presence of numerous pillows showing hydrothermal variolites (Fig. 4d) crops out below. The metamorphic grade is low, as only few tuffs show the development of green-blue amphiboles. This unit can thus probably be assigned to OC1. Farther to the south, the same type of chaotic unit as mentioned above is underlain, via a ~50 m long serpentinite body, by a glaucophane–lawsonite-bearing unit resembling OC2. The Afyon zone crops out just beneath, as attested by the presence of platy limestone underlain by albite and chlorite-bearing schists (Kaya et al., 1995; Pourteau, 2011).

A second section to the east shows a ~500 m thick slice of amphibolitic rocks at the base of the peridotite overlain by unconformable Palaeogene basin deposits (Fig. 5e). This metamorphic sole could be traced to the south under the ophiolitic body for 2–3 km and tectonically overlies the accretionary complex. The complex is locally made of tuffs, mafic lavas, pillow basalts, radiolarian chert and pelagic limestone, with only low-grade mineral assemblages equivalent to OC1. Coherent, hm-scale tectonic slices were again recognised, as underlined by the presence of metric serpentinite zones in between the slices. As in other localities where OC1 and OC2 were investigated, no penetrative deformation has been observed. The Afyon zone is found just below, as attested by the presence of a major contact, and platy limestone (Kaya et al., 1995).

4.7. Devlez area

Almost the full continental sequence (İnönü and Devlez units) crops out in the Devlez area, with large exposures of mafic blueschists and metacherts that are characteristic of the latter unit. A seemingly concordant, stratigraphic contact between the İnönü marbles and the Devlez unit can be observed in a few places, marked by a dm-scale calcschist level in between. Deformation patterns were investigated in both the metatuffs and metacherts. Stretching lineation shows two main directions, around N130–N160 or N015. Fold axes show a unimodal distribution with a NW–SE direction corresponding to the main stretching lineation, as observed by Okay (1980a). Large-scale folds in the metabasites have the same NW–SE axis as the hm-scale fold in the marbles south of Ketenlik (Figs. 2b,c,3f). The Devlez formation is tectonically overlain by the accretionary complex. As for other areas, two distinct accretionary units can be recognized. South of Ketenlik a klippe of OC1, described by Okay and Whitney (2010), is clearly delimited by a serpentinite zone. This klippe rests on top of OC2. At the basis of OC2 was found one zone with metasomatic rocks consisting of lawsonite-bearing chloritite, with minor sodic pyroxene and titanite. To the north, the Devlez formation probably crops out under OC2, but this is poorly constrained due to poor outcrop. Near Çayıroluk OC2 shows an alternation of green to blue metatuffs, cherts with more pelitic Fe–Mg carpholite-bearing levels, and locally massive, dm-scale blocks of blue pillow basalts and pillow breccias displaying relict magmatic pyroxenes. Southwards, OC1 overlies OC2 and displays red radiolarian cherts, pillow basalts, aragonitised limestones (Topuz et al., 2006; Fig. 4e) and green (meta)tuffs. No metamorphic sole was found below the main ophiolitic body.

5. New mineralogical and petrological constraints on the metamorphic evolution of the tavşanlı zone

The Tavşanlı zone hosts extensive outcrops of HP–LT mineral assemblages (Cogulu, 1967; Lisenbee, 1972; Okay, 1980a, 1980b; Okay, 1982; Van der Kaaden, 1966). New occurrences are reported below, with a special focus on the accretionary complex and parts of the Orhaneli unit that were not investigated so far, among which the Kocasu formation in the regions of Köseler, Tekerler, Dutluca, or the Devlez formation of Domaniç, and Köseler (Fig. 2c). The metamorphic soles were also investigated, providing new evidence of HP overprint of sub-ophiolitic metamorphism. The first PT estimates for the accretionary complex, as well as the first T_{max} based on the Raman spectroscopy of carbonaceous material, are provided in the last paragraph.

5.1. Methods

5.1.1. Electron-microprobe analysis

All electron-microprobe analyses were carried at CAMPARIS (University Paris 6) using either SX100 or SX Five instruments. Classical analytical conditions were adopted (15 kV acceleration voltage, 10 nA beam current, 2–3 μm beam size, wavelength-dispersive spectroscopy mode). Albite (Na), diopside (Mg, Si, Ca), orthoclase (Al, K), $MnTiO_3$, Fe_2O_3 (Fe) and Cr_2O_3 (Cr) were used as standards for the relevant. Additional observations were made using a Zeiss Σigma Scanning Electron Microscope at Laboratoire de Géologie, Ecole Normale Supérieure, Paris.

5.1.2. Raman spectroscopy on carbonaceous matter

All Raman spectra on carbonaceous material were obtained using a Renishaw inVia Spectrometer at Laboratoire de Géologie, ENS. A 514 nm argon laser in circular polarisation was used. The Laser was focused on the polished thin section sample (cut in the XZ plane of deformation) using a Leica microscope with a 100× objective. Laser power was set a 10% of 20 mW. Carbonaceous matter was analysed below a transparent mineral, generally quartz. Between 10 and 25 spectra per sample were acquired in the extended scanning mode 1000–2000 cm^{-1} with an acquisition time of 30 to 60 s and 1–3 accumulation, using the calibration method of Beyssac et al. (2002, 2003). Spectra were then processed following the procedure described by Beyssac et al. (2003). This thermometer allows an accuracy of ±50 °C in the range of 350–650 °C (Beyssac et al., 2002).

5.1.3. Thermodynamic modelling

PT pseudosection modelling (i.e., predicting phase diagram for a fixed bulk composition) was carried out in the simplified system KFMASH (K_2O–FeO–MgO–Al_2O_3–SiO_2–H_2O) using Perple_X 6.6.8 (Connolly, 2005, 2009; Connolly and Kerrick, 1987) and the thermodynamic database of Holland and Powell (1998) with recent updates. Solution models are after Holland et al. (1998) for chlorite, after Coggon and Holland (2002) for phengite, and after Holland and Powell (1998) for chloritoid and carpholite.

5.2. Distribution of HP minerals: Orhaneli unit

The distribution of the (rather uncommon worldwide) paragenesis lawsonite + chloritoid + jadeite + glaucophane described by Okay (2002) was extended further to the east in the Orhaneli unit (Fig. 2). Sample OR1024 (Fig. 6a) is one of the best-preserved samples and preserves an undeformed texture, as for most greyschist samples in fact.

Greyschists with the assemblage jadeite + lawsonite were found near Dutluca, as mentioned earlier (sample 11TAV15). In the region of Elmaağacı, schists bearing jadeite + lawsonite were found under the marbles, near the village of Köseler and might represent equivalents to the Kocasu formation.

The Tekerler region shows jadeite + glaucophane ± lawsonite greyschists alternating with lawsonite–glaucophane-bearing quartzite.

Northwest of Dursunbey jadeite or chloritoid + lawsonite bearing schists were also found alternating with lawsonite + glaucophane mafic blueschists. The alternation of greyschists with mafic material was not studied in detail however. This part of the Orhaneli unit was interpreted as the basement of the Tavşanlı zone (Özbey et al., 2010, 2013a,3b).

Throughout the study area, mineral compositions show only small variations: the XMg (XMg = Mg/(Fe + Mn + Mg) of chloritoid ranges between 0.1 and 0.2 (Fig. 7a; Table 1). Clinopyroxene is almost pure jadeite (Fig. 7b; Table 1). Blue amphibole formula units, calculated following the procedure described in Leake et al. (1997), indicate a composition between glaucophane and ferro-glaucophane (Fig. 7c; Table 1). Silica content in phengite varies between 3.4 and 3.6 p.f.u (per formula unit), mostly along the tschermak (i.e., Si,(Fe,Mg) = 2Al) and pyrophyllitic (i.e., Si = Al,K) solid solutions (Fig. 7d; Table 1).

Another typical paragenesis is glaucophane + lawsonite. It was mainly found in metabasites and metatuffs of the Devlez formation (Figs. 3e, 6b; Okay, 1980a). Sample 11TAV33 is a well-foliated metabasite, with glaucophane + lawsonite containing up to 90% of the mineral mode (Fig. 6b). In addition to glaucophane + lawsonite, the presence of phengite, sodic pyroxene, chlorite, titanite was also noticed (Okay, 1980a, 1980b). Magmatic augite is found in some pillows

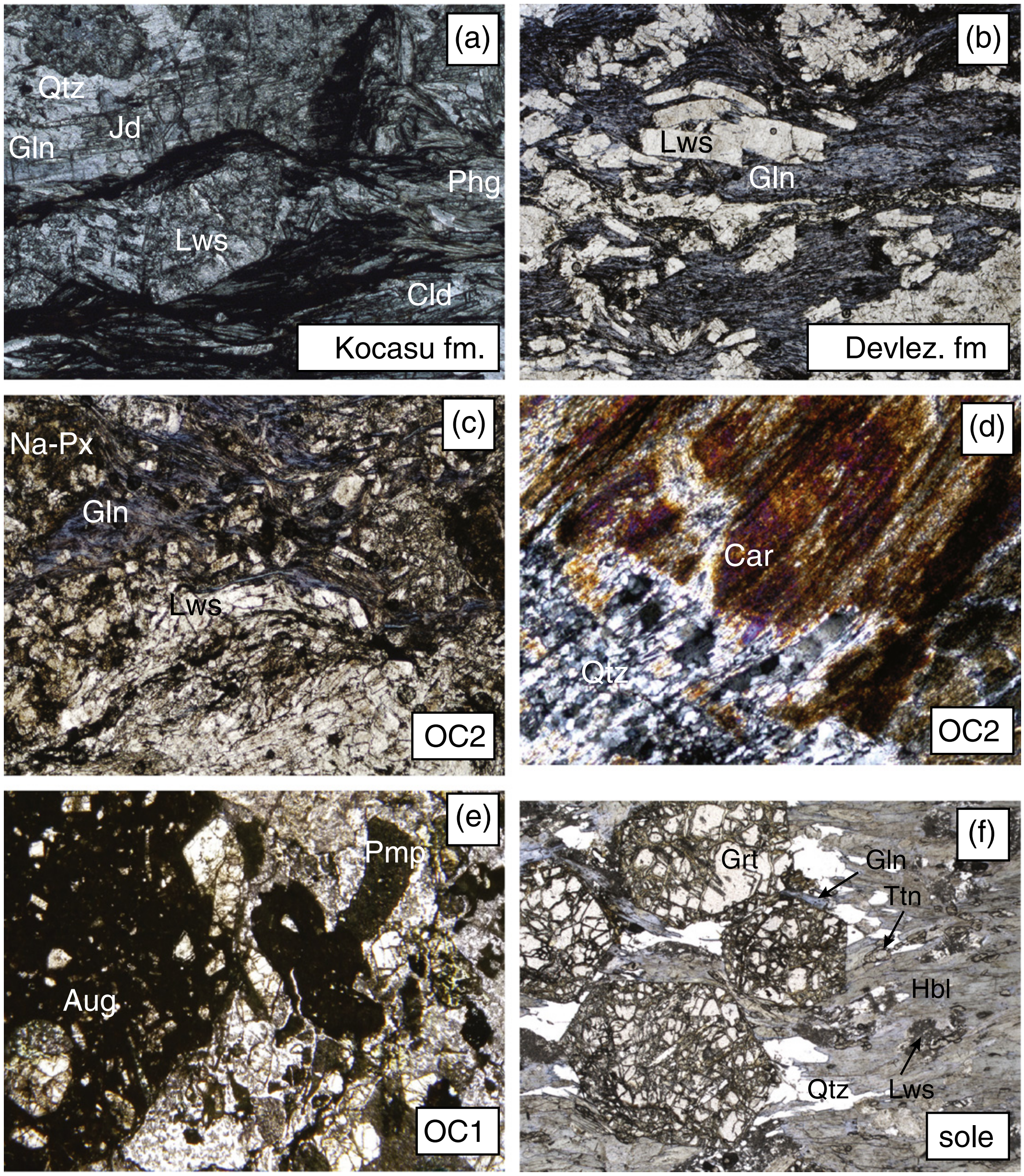

Fig. 6. Microphotographs of selected samples. (a) Typical greyschsit of the Orhaneli area, Plane Polarised Light (PPL); (b) Typical high pressure metabasite of the Devlez formation, PPL; (c) Typical high pressure metabasite of the OC2, PPL; (d) Fe–Mg carpholite bearing quartzite of the OC2, Cross Polarised Light; (e) Typical massive lava of the OC, with pristine Augite, and incipient metamorphic mineral as pumpellyite, chlorite, tiny phases and aggregates, PPL) (f) Metamorphic sole from Elmaağacı, with initial grt + hbl paragenesis, and the high-pressure overprint showing gln rims and lws aggregates.

or pillow breccia as metastable relics, as highlighted by the associated glaucophane + lawsonite recrystallized matrix. Glaucophane + lawsonite are also common in garnet-phengite bearing metacherts. Northwest of Domaniç, an equivalent to the Devlez formation was found on top of the marbles, showing an alternation of mafic rocks and metachert with similar assemblages. The Devlez formation, showing glaucophane + lawsonite with minor sodic pyroxenes was also found on top of the marbles in the Elmaağacı–Köseler region (Fig. 5b). In all the Devlez formation, sodic amphiboles shows compositional variation, with the development of ferric end-members (Fig. 7c; Amphibole with composition between ferro-glaucophane, glaucophane and corresponding ferric equivalent (Leake et al., 1997; Fig. 7c; Table 1). Sodic pyroxene generally has a composition of aegirine–augite or aegirine, with rare occurrences of true omphacite or aluminous pyroxenes (Fig. 7b). As in the Kocasu formation, phengite displays about 50 mol% of celadonite component corresponding to 3.4 to 3.6 Si p.f.u with 10 mol% of pyrophyllite end-member (Fig. 7d; Table).

5.3. Distribution of HP minerals in the accretionary complex: OC2 vs. OC1

The accretionary complex was separated on the basis of high-pressure mineral occurrences. OC2 shows typical sub-blueschist to blueschist-facies metamorphism, whereas complex 1 shows non-metamorphic assemblages to incipient blueschist facies assemblages. Mineral assemblage and their relative metamorphic grade are shown on Fig. 2. OC1 and OC2 also differ in terms of lithology. Although both are made of oceanic crustal and mantle rocks, radiolarian cherts dominate in OC1, whereas only rare occurrences were found in OC2. Pillow lavas are generally best preserved in OC1 (Fig. 4d,e).

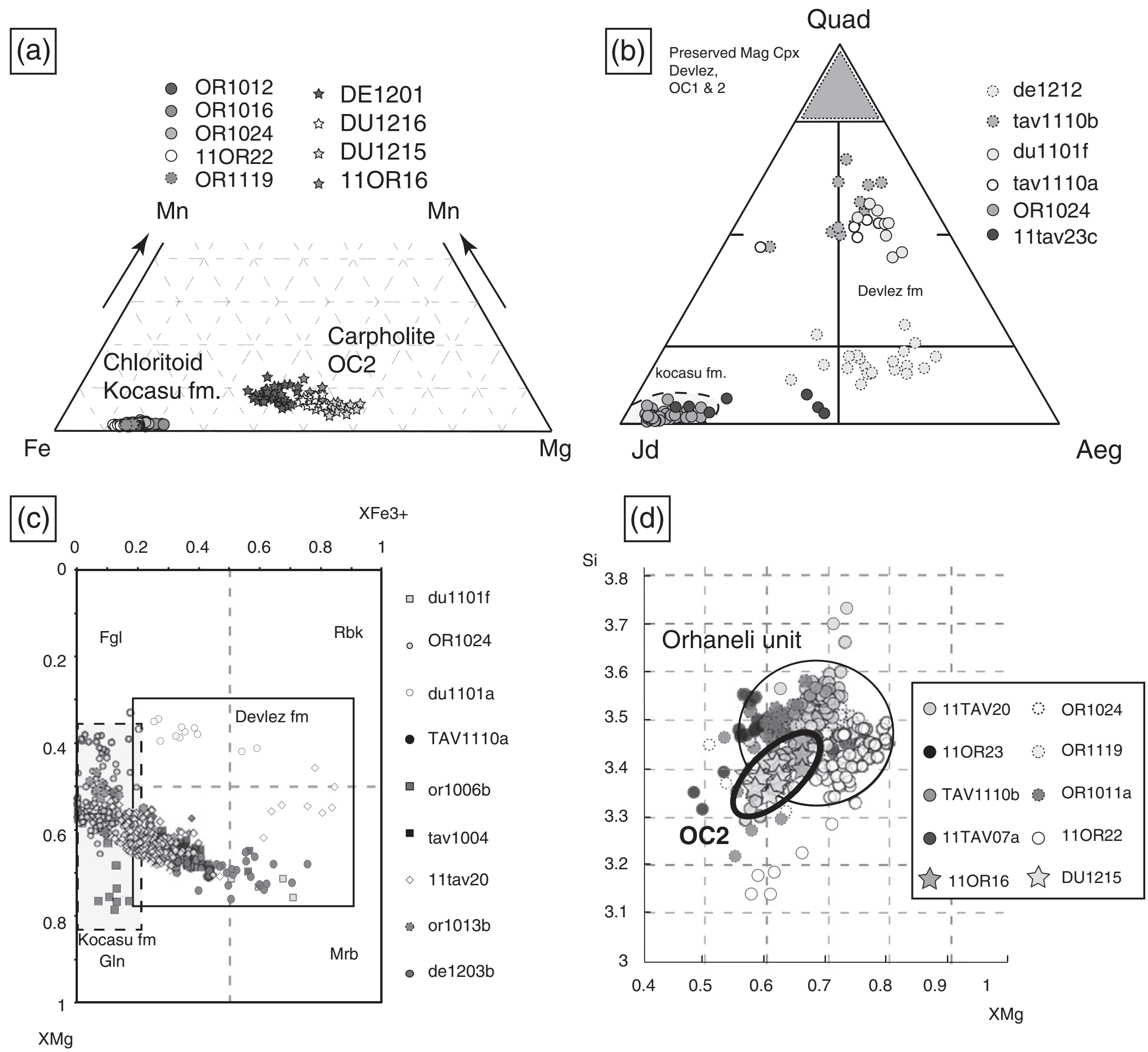

Fig. 7. Representative microprobes analysis of (a) Chloritoid and Carpholite; (b) Clinopyroxenes; (c) Sodic amphiboles (d) Phengite.

In OC2, metabasite and metatuffs display the blueschist-facies lawsonite + glaucophane ± sodic pyroxene assemblage (11OR16b; Fig. 6c). The association of sodic pyroxene + lawsonite + chlorite assemblage was also found, though less commonly. This assemblage was interpreted as sub-blueschist or blueschist facies showing a different assemblage due to variations in bulk compositions (Vitale-Brovarone et al., 2011; Wei and Clarke, 2011) or oxidation state (Diener and Powell, 2012). When present, sodic pyroxene is characterised by high ferric content ($XFe^{3+} = Fe^{3+}/(Al^{3+} + Fe^{3+}) > 0.5$; Fig. 7b). Relict magmatic pyroxene (Okay, 1980a,b), as in the Devlez formation, is found as inclusions in the glaucophane + lawsonite matrix (Fig. 7b). Fe–Mg carpholite bearing quartzite was found in several places (Figs. 4a,b, 6d). It is interbedded in the metatuff and metabasite and might represent cherts with a very local higher pelitic component. At the thin section scale (Fig. 6d) Fe–Mg carpholite is present as large prisms and fibres in a quartz-rich rocks (impure quartzite or locally quartz veins). Its composition varies from one sample to another, with XMg between 0.4 and 0.6 (Fig. 7a; Table 1). Chlorite and phengite are present in minor amounts at textural equilibrium.

OC1 shows poorly metamorphosed rocks (Fig. 6e). Some mafic samples show a doleritic texture, with a paragenesis consisting of chlorite, albite replacing magmatic plagioclase, aegirine–augite or aegirine pseudomorphs after magmatic augite (Okay, 1982). Some pillow breccias were found that contain magmatic augite with narrow reaction rims of aegirine–augite. Magmatic augite coexists with rare, tiny, highly ferric lawsonite crystals (Table 1). Chlorite, phengite, carbonate and other low-grade minerals such as pumpellyite or albite were also observed (Fig. 6e). Those mineral assemblages match with the predicted sub-blueschist assemblage modelled by Massonne and Willner (2008) for MORB composition. The only difference is that no amphibole (neither Ca- nor Na-bearing) and no stilpnomelane were observed in the mafic schist of OC1. Contrary to OC2, no occurrence of sodic amphibole or Fe–Mg carpholite was found (see also Okay, 1982).

5.4. Distribution of metamorphic soles

The non-metamorphic obducted peridotite is found regionally, except on the Kocasu cross section (Fig. 5a). A garnet-bearing amphibolite-facies metamorphic slice was found at the base of the peridotite. It crops out near Çivili as a ~100 m thick slice (Figs. 2c,4f; Okay et al., 1998). The petrology of the amphibolite slice of the Çivili area described by Okay et al. (1998) will serve here as a reference. Amphibolite-facies assemblage is hornblende + plagioclase (mainly replaced by albite) + epidote +

Table 1
Representative EPMA analysis for chloritoide, clinopyroxene, amphiboles, phengites, lawsonite and carpholite. FeO in lawsonite assumed as Fe_2O_3.

	Kocasu formation						Devlez formation					OC2			Sole				OC1
Mineral sample	cld	jd	gln	gln	phg	lw	lw	gln	gln-rbk	mrb	phg	car	car	phg	hbl core	gln rim	rbk	Aeg	lws
	OR1024	OR1024	OR1024	OR1024		OR1006B	11TAV20	11TAV20	11TAV20	11TAV20	11TAV20	DU1215	11OR16	11OR16	OR1028A	OR1028A	11TAV13b	11TAV13B	du1101A
Analyse	*45*	*35*	*47/1,*	*36/1,*	*18*	*b38*	*114/1.*	*1331*	*1335*	*1343*	*77*	*16/1.*	*6/1.*	*82*	*3/62.*	*18/15,*	*128/1.*	*116*	45/1
SiO2	24.468	59.615	57.126	58.449	52.232	37.920	38.690	57.535	55.765	55.280	52.520	38.570	37.699	48.660	43.800	55.465	51.738	53.491	37.030
TiO2	0.000	0.019	0.116	0.000	0.005	0.290	0.335	0.119	0.084	0.033	0.112	0.000	0.238	0.064	0.610	0.000	0.329	0.137	0.150
Al2O3	41.391	0.003	11.534	12.081	26.253	31.870	31.380	9.549	7.534	2.405	22.562	30.705	30.991	25.708	13.385	10.039	2.900	5.017	29.420
Cr2O3	0.084	23.048	0.000	0.000	0.025	na.	na.	0.000	0.069	0.034	0.181	na	na	0.099	0.026	0.053	0.029	0.000	0.000
FeOtot	24.389	2.941	15.748	11.946	2.609	0.280	1.191	13.153	14.461	22.225	3.813	10.836	9.946	3.866	14.171	15.985	33.242	23.787	2.310
MnO	0.541	0.065	0.015	0.044	0.006	0.020	0.000	0.214	0.251	0.307	0.051	1.082	1.381	0.276	0.026	0.142	0.174	0.081	0.020
MgO	2.159	0.144	6.258	8.205	3.661	0.020	0.000	9.158	10.061	8.279	4.358	6.384	6.625	4.096	10.195	6.302	0.520	0.176	0.020
CaO	0.020	0.255	0.067	0.012	0.000	17.010	17.379	0.801	1.773	1.526	0.108	0.001	0.012	0.114	9.981	0.668	0.188	1.604	17.030
Na2O	0.017	14.270	7.131	7.109	0.236	0.020	0.019	7.065	6.520	6.158	0.166	0.000	0.019	0.130	2.861	6.681	6.507	12.524	0.020
K2O	0.011	0.001	0.002	0.006	10.452	0.000	0.017	0.036	0.035	0.016	11.001	0.000	0.016	9.916	0.321	0.045	0.065	0.000	0.000
total	93.078	100.361	97.996	97.852	95.481	87.430	89.013	97.629	96.554	96.264	94.870	87.578	86.926	92.929	95.376	95.380	95.691	96.816	86.000
Si	2.007	2.030	7.958	8.003	3.473	2.007	2.023	7.982	7.874	8.043	3.559	2.046	2.011	3.364	6.535	7.992	7.993	2.024	2.022
Ti	0.000	0.000	0.012	0.000	0.000	0.012	0.013	0.012	0.009	0.004	0.006	0.000	0.010	0.003	0.068	0.000	0.038	0.004	0.006
Al	4.001	0.925	1.894	1.950	2.057	1.988	1.934	1.561	1.254	0.412	1.802	1.920	1.949	2.094	2.353	1.700	0.528	0.224	1.893
Cr	0.005	0.000	0.000	0.000	0.001	na	na	0.000	0.008	0.004	0.010	na	na	0.005	0.003	0.006	0.004	0.000	0.001
Fe2/Fetot	1.673	0.084	1.616	1.215	0.145			1.220	1.063	1.429	0.216	0.481	0.444	0.223	1.413	1.700	1.382	0.113	
Fe3			0.219	0.153		0.012	0.052	0.306	0.645	1.276		0.080	0.051		0.355	0.224	2.913	0.640	0.105
Mn	0.038	0.002	0.002	0.005	0.000	0.001	0.000	0.025	0.030	0.038	0.003	0.049	0.062	0.016	0.003	0.017	0.023	0.003	0.000
Mg	0.264	0.007	1.300	1.675	0.363	0.002	0.000	1.894	2.118	1.796	0.440	0.505	0.527	0.422	2.268	1.354	0.120	0.010	0.002
Ca	0.002	0.009	0.010	0.002	0.000	0.965	0.974	0.119	0.268	0.238	0.008	0.000	0.001	0.008	1.596	0.103	0.031	0.065	0.996
Na	0.003	0.000	1.926	1.887	0.030	0.002	0.002	1.900	1.785	1.737	0.022	0.000	0.002	0.017	0.828	1.867	1.949	0.919	0.002
K	0.001	0.942	0.000	0.001	0.886	0.000	0.001	0.006	0.006	0.003	0.951	0.000	0.001	0.874	0.061	0.008	0.013	0.000	0.000
Xprl					0.083						0.024			0.105					
Xmu					0.457						0.369			0.479					
Xcel					0.391						0.545			0.270					
XFe	0.847																		
XMn	0.019																		
XMg	0.134		0.446	0.580				0.608	0.666	0.557		0.512	0.510		0.616	0.443	0.039		
XFe3			0.106	0.073				0.166	0.364	0.756					0.286	0.117	0.726		
Jd		0.949																0.235	
Aeg		0.000																0.670	
Quad		0.050																0.093	

Table 2
Peak temperature obtained by RSCM. SD, standard deviation; n, number of spectral acquisitions; SE, standard error, which is SD divided by SQRT(n); RSCM, Raman spectroscopy of carbonaceous matter.

Sample	n	Av. T(°C)	SD	SE
11OR19	11	478	24	7
OR1024	17	538	25	6
OR1006b	19	515	31	7
OR1011a	20	498	29	7
OR1012	16	540	16	5
OR1013b	18	556	26	6
OR1014a	19	553	30	7
OR1119	22	493	20	4
OR1120	18	483	23	5
OR1121	12	499	18	5
OR1123b	19	553	28	6
OR1124	18	543	25	6
OR1140	20	529	29	7
TU1015	20	467	27	6

quartz + rutile ± garnet ± opaque. This slice is interpreted as the metamorphic sole of the ophiolite. An incipient blueschist facies was noticed for this amphibolitic slice, and was also described in some other amphibolitic soles by Gautier (1984), Önen and Hall (1993) and by Dilek and Whitney (1997) in the Sivrihisar region, north of Kütahya and the Mersin region, respectively. Outcrops of metamorphic sole were also found near the village of Elmaağacı, and south of Tavşanlı, near the village of Karacakaş (Figs. 5c,e). Both of them show a blueschist-facies overprint marked by glaucophane rims on hornblende and lawsonite growth in plagioclase (Fig. 6f; Table 1; Plunder et al., 2013). South of Tavşanlı, the amphibolitic sole shows the development of aegirine-like clinopyroxene and riebeckite (Table 1). In most samples, plagioclase is destabilised in aggregate or needles of lawsonite in coarse albite. Epidote, whenever present, is part of the original assemblage as attested by inclusions in garnet. The presence of glaucophane + lawsonite ± sodic pyroxene attests that PT conditions of metamorphic soles changed during their history, from amphibolite-facies to lawsonite blueschist-facies conditions.

5.5. Preliminary PT estimates

This section provides the first T_{max} estimates for the continental units of the Tavşanlı zone and, based on the finding of Fe–Mg carpholite, the first PT estimates for the OC2 accretionary complex.

5.5.1. Raman spectroscocopy on carbonaceous material (RSCM)

This thermometric method provides maximum temperature estimates (T_{max}) for carbonaceous-rich samples, based on the irreversible transformation of organic matter (Beyssac et al., 2002). Samples of the Kocasu formation are particularly suitable for RSCM as they contain abundant carbonaceous matter. T_{max} were determined for 12 greyschist samples from the Kocasu formation in the region of Orhanli unit (Fig. 2b). Two other samples were also selected for preliminary study of Kocasu and Köseler region. T_{max} estimates range between 470 and 550 °C (Fig. 2c; Table 2) and yield slightly higher temperature estimates than those proposed before on the basis of the absence of garnet (Okay, 2002).

5.5.2. Pseudosection modelling

Sample 11OR16 (OC2, Kocasu region, Fig. 2c) is an impure quartzite containing Fe–Mg carpholite, chlorite and phengite. Water was considered in excess for pseudosection modelling, as suggested by the large amount of hydrous phases (>50% of the mode is represented by Fe–Mg carpholite, chlorite or phengite). Other elements such as TiO_2, CaO, Na_2O, MnO, Cr_2O_3, Fe_2O_3 were neglected given the mineral chemistry of this sample and their respective minor amount as part of the bulk compostion. Observed Fe–Mg carpholite have XMg between 0.5 and 0.54 (Fig. 7a) and the Si content of phengite is 3.35–3.40 p.f.u (Fig. 7d; Table 1). Considering that the estimated pyrophyllite component accounts for 0.1 to 0.15 of the Si p.f.u. of phengite, modelled silica contents must be in the range of 3.25 and 3.30. Together with the observed XMg of Fe–Mg carpholite, the pseudosection leads to PT conditions for the high-pressure unit (OC2) of the oceanic accretionary complex of 11 to 13 kbar and 250 to 350 °C (Fig. 8a).

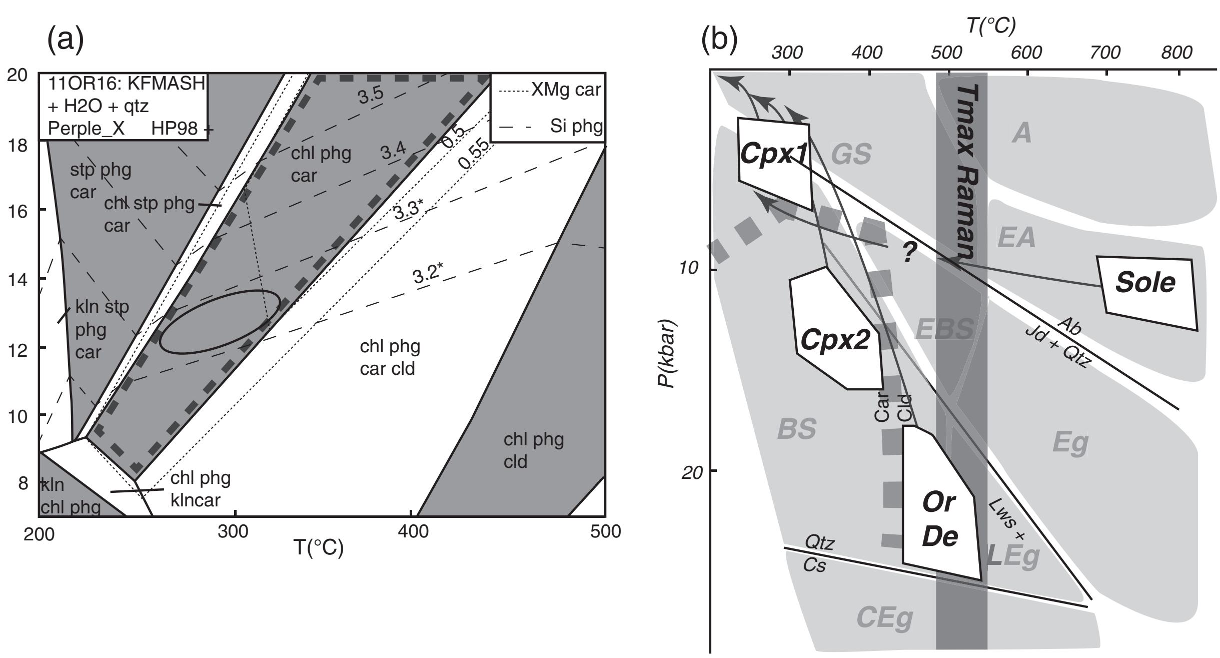

Fig. 8. (a) PT pseudosection computed in the system KFMASH using Perple_X 6.6.8, with solution models given in text. Si isopleth p.f.u in phengite and XMg in carpholite give the PT condition for sample 11OR16. (b) Compilation of available and determined PT conditions for the different units of the Tavşanlı zone. Mineral abbreviation after Kretz (1983) except for car: carpholite.

6. Interpretations and discussion

6.1. Tectono-metamorphic evolution the Tavşanlı zone

Fig. 2 demonstrates the occurrence of diagnostic, HP–LT minerals throughout the western part of the Tavşanlı zone. In particular, extensive T_{max} estimates for the continental-derived Kocasu formation are homogeneous across a vast area (Figs. 2b,c) and are systematically slightly higher (>470 °C) than previous temperature estimates (430 ±30 °C; Okay, 2002). Preliminary pseudosection calculations also point to the consistency between PT estimates and T_{max}. Small variations in T_{max} could relate to additional heat from nearby granodiorite intrusions (Fig. 2), but do not change the general trend: the thermal regime of continental subduction is higher than previously reported (Okay, 2002).

Deformation patterns of the continental Kocasu formation shows similar, parallel stretching lineations, trending NNE–SSW to NE–SW across a large area (Figs. 2a,c), attributable to peak burial conditions. All tectonic measurements (i.e., from sheath folds, drag folds, stretching lineations, boudinaged structures) were performed on metre-scale structures or smaler. No major tectonic thrusts or duplications were observed in the continental units, and only decametre-scale folds were found in the Orhaneli unit. Rare hectometre-scale open folds with EW trending axes (Fig. 4b) characterize the İnönü marble. However, no reliable deformation criteria were found in this formation, despite earlier claims of E–W trending stretching lineations (Lisenbee, 1972). The combination of homogeneous PT and coherent lineations within the Kocasu formation on a regional-scale (i.e., >100 km), together with the lack of tectonized contact at the interface of the Kocasu/İnönü/Devlez formations, suggests that the Orhaneli unit was buried at similar depths and exhumed coherently, as a fairly rigid body.

In the Sivrihisar greyschist unit, which represents a lateral equivalent to the Orhaneli unit (Okay and Whitney, 2010), relict high-pressure mineral assemblages containing glaucophane, lawsonite, chloritoid and/or jadeite were observed in the northern part of the unit (Çetinkaplan et al., 2008; Gautier, 1984). Radiometric ages for high-pressure metamorphism (Ar–Ar and Rb–Sr on phengite; 80 Ma; Sherlock et al., 1999; Seaton et al., 2009) and stretching lineations (N–S to NW–SE) are the same as in the Orhaneli area. Reequilibration under greenschist-facies conditions during exhumation was nevertheless more thorough in the Sivrihisar region (Gautier, 1984; Monod et al., 1991).

Deformation patterns in the Devlez formation, which corresponds to the upper part of the Orhaneli unit, are slightly different with a dominant N160 (and to a lesser extent N15–N20) trending stretching lineation. The Devlez formation shows a sparse outcropping (20 × 15 km) in the large Tavşanlı zone (250 × 50 km) whereas the Kocasu and Inonü formations, or their equivalents, crop out extensively (Fig. 2a, c). The local presence of the Devlez formation may thus correspond to an inherited palaeogeographic feature, marked by volcanism in a radiolarian basin on the very distal part of the thinned continental margin. In fact, the İnönü marble formation too shows a strongly variable thickness in the different investigated areas, from a few metres to few kilometres. Local variations in palaeogeography and/or subsidence, rather than differential erosion, thus probably account for the respective facies and thickness variations in both the Devlez and İnönü formations.

Two different ocean-derived accretionary complexes sandwiched between the Orhaneli unit and the overriding ophiolite (OC1 and OC2) were recognized in the study area. OC1 corresponds to a poorly-metamorphosed series of imbricates made of crust and cover showing little internal deformation, which were essentially statically recrystallized under low-grade blueschist-facies conditions. Observations demonstrate that this unit, so far loosely referred to as mélange formed in a subduction channel (Kaya, 1972; Lisenbee, 1972; MTA, 2002), is not a random mafic and sedimentary mélange within a serpentinite matrix as suggested by Okay (1982). Observed mineral assemblages (i.e., lawsonite with 5% Fe_2O_3, aegirine and aegirine–augite pyroxene; Fig. 7b) and the absence of higher-grade metamorphic minerals such as glaucophane, jadeite–omphacite or of the higher-pressure Fe–Mg carpholite allow to bracket PT estimates within the range of 4–8 kbar and 250–300 °C (Fig. 8b), in line with previous estimates (Okay, 1982; Topuz et al., 2006). OC2, by contrast, is a strongly recrystallized blueschist-facies unit containing both pelitic and mafic index minerals (i.e., Fe–Mg carpholite and the assemblage glaucophane + lawsonite ± sodic pyroxene, respectively). PT estimates obtained through pseudosection modelling indicate conditions of 10–15 kbar and 300–400 °C (Fig. 8a). Similar mineral compositions in the various exposures indicate that these PT conditions prevailed, at least as a first approximation, for the entire OC2.

A systematic, static glaucophane–lawsonite blueschist-facies overprint was observed on the metamorphic sole (as earlier observed, locally, by Gautier, 1984; Önen and Hall, 1993; Dilek and Whitney, 1997; Okay et al., 1998). Metamorphic soles are generally regarded as having formed during subduction inception, by the accretion of oceanic crustal material beneath the still hot upper-plate mantle (Spray, 1984; Wakabayashi and Dilek, 2003). The existence of such ubiquitous HP–LT overprint suggests that the metamorphic sole was either (1) exhumed and later subducted again in a cold regime (Dilek and Whitney, 1997; Wakabayashi, 1990) along with the OC1–2 and Orhaneli units, or (2) directly refrigerated after amphibolitisation, as a result of cooling of the subduction gradient (~10 °C/km; Peacock, 1996; van Keken et al., 2011). The static overprint, the lack of displacement of the sole with respect to either the ophiolite or the oceanic complexes, the lack of metamorphic sole fragments and/or boudins in the complexes, strongly support the second hypothesis.

HP–LT metamorphism in the Tavşanlı zone thus ranges from incipient metamorphism to high-pressure blueschist-facies conditions with pressure gaps (Fig. 8b) coinciding with major tectonic contacts (i.e., from bottom to top: Orhaneli/OC2, OC2/OC1, OC1/metamorphic sole). Incidentally, the PT conditions of the lawsonite-bearing eclogites of Halibağı (~26 kbar–500 °C; Davis and Whitney, 2006) can even be extended to the Orhaneli unit (Kocasu formation, ~22 kbar–520 °C). Nevertheless unknowns remain: the lawsonite eclogite of Halibağı might be (i) an equivalent to the Devlez formation, but decoupled from the underlying marble formation; (ii) an oceanic accretionary unit detached at similar depth as the continental units.

Such constant features along the strike of the Tavşanlı zone point to similar dynamics of continental subduction below an oceanic lithosphere across a vast area (250–300 km). Cooling and blueschist overprinting of the metamorphic sole takes place rapidly, about 5 My after intra-oceanic subduction initiation (at *ca.* 95–90 Ma; Önen and Hall, 1993, 2000; Okay et al., 1998; Dilek et al., 1999) as HP–LT metamorphism is documented at 85–80 Ma in the Orhaneli unit (Sherlock et al., 1999). The results suggest that the exhumation of Tavşanlı HP–LT rocks, at 85–80 Ma, takes place through a Chemenda-type, rigid, buoyancy-driven exhumation (Chemenda et al., 1996; Okay et al., 1998). Exhumation of the Tavşanlı zone is constrained at ~85–70 Ma (Çetinkaplan et al., 2008; Monod et al., 1991; Seaton et al., 2009; Whitney and Davis, 2006). It occurs in any case prior to 60 Ma, as shown by zircon fission-track ages (Thomson and Ring, 2006), cross-cutting Eocene calc-alkaline magmatism, tentatively related to slab breakoff (Altunkaynak, 2007; Dilek and Altunkaynak, 2009) or roll-back/steepening (van Hinsbergen et al., 2010). The absence of discontinuity on tomographic images and the presence of lower Lutetian neritic and Ypresian limestones unconformably covering both the ophiolite and accretionary complex (Baş, 1986; Özgen-Erdem et al., 2007; Servais, 1981, 1982) rather support the second hypothesis.

6.2. Implications for accretion/exhumation and mechanical coupling

Oceanic complexes OC1 and OC2 found in the Tavşanlı zone reveal a simple, non-random structural organisation (contrary to subduction tectonic melanges marked by the existence of reworked material in a matrix; Cloos, 1982; Cloos and Shreve, 1988b; Festa et al., 2012;

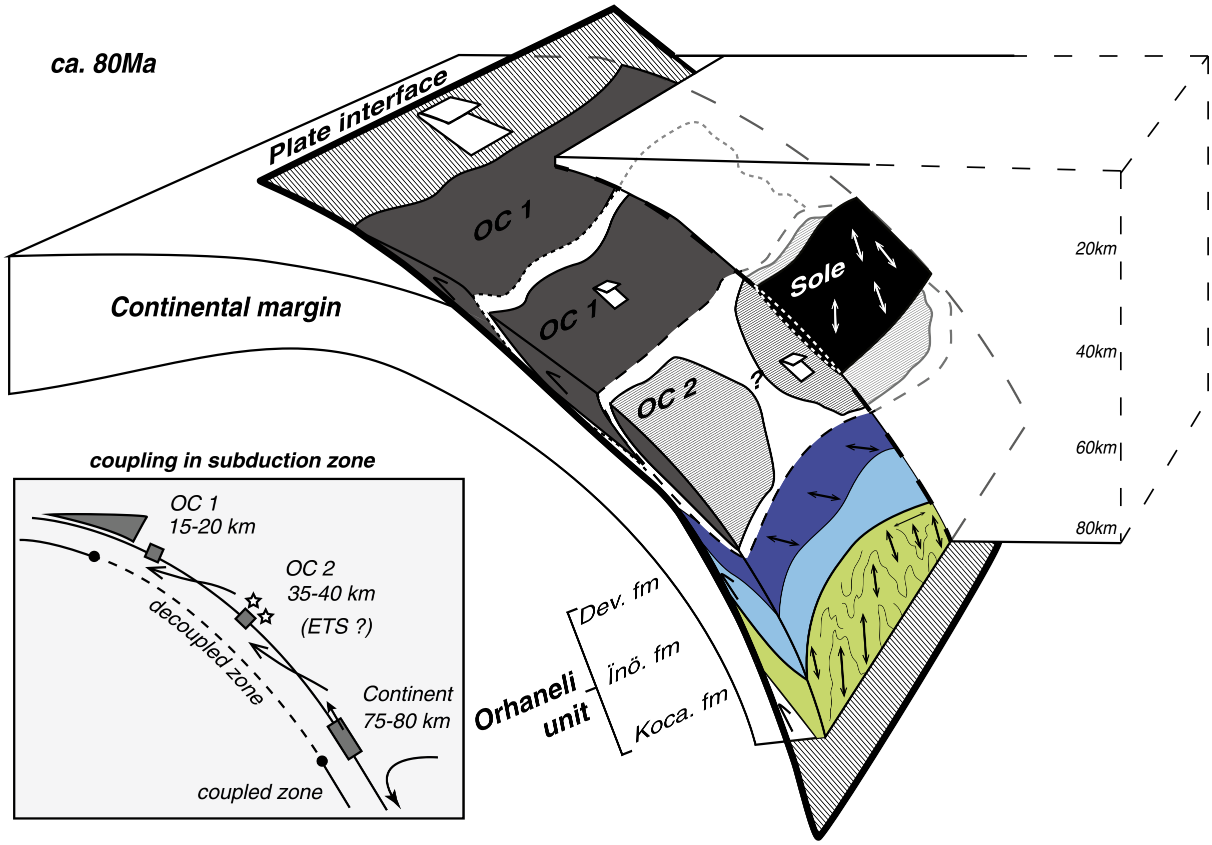

Fig. 9. Block diagram of the plate interface during continental subduction at 80 Ma. Coupling and decoupling depths from Wada and Wang, (20090) and Syracuse et al (2010). Lineation measured in various units is reported as double arrows.

Wakabayashi, 2011), made of a stack of tectonic slices imbricated at different scales. Laterally continuous slices show alternating layers of lightly metamorphosed basalts, cherts and minor tuffs. This can be observed at the scale of the outcrop (Dutluca, Tekerler and Kocasu sections) as well as at the scale of several hundred metres and up to the kilometre-scale (Fig. 5a,b,c,), the largest imbrication scale being the one separating OC1 and OC2. Deformation patterns depend on the depth at which the unit was buried: the very low-grade OC1 shows very low internal deformation, whereas higher-grade OC2 shows pervasive deformation patterns comparable to the continental-derived Orhaneli unit.

Respective thicknesses are less than a kilometre for OC1 (about ~500 m on the cross sections) and ~100–200 m for OC2. Incidentally, the low sediment fraction (other than radiolarian cherts) observed in both accretionary units suggests that the intra-oceanic subduction was sediment-starved and thus far from both the Anatolide–Tauride and Sakarya continental margins.

Oceanic complexes OC1 and OC2 are thus interpreted as fragments of subducting oceanic crust and related volcanoclastic or pelagic cover scraped off and accreted/underplated at the bottom of the upper plate at depths of ~15–20 km (OC1) and ~40 km (OC2) along the plate interface (Fig. 9). The considerable thickness of OC1 in the Kocasu section (~1 km; Fig. 5a) suggests that some of the exhumed material could correspond to ocean-floor asperities or seamounts. The lack of gabbros in these accretionary complexes suggests that they derive from the scraping of shallow material of the downgoing plate (i.e., the hydrothermalised section). The structure and PT conditions estimated for the oceanic accretionary complexes of the Tavşanlı zone compare well with other such complexes in the Nankai trench, the Chugah complex in Alaska, the Franciscan, the Makran or the Schistes Lustrés in the Western Alps (Festa et al., 2012; Kimura, 1994; Kopp et al., 2000; Kusky et al., 1997; Platt, 1986; Plunder et al., 2012).

Slices of the upper oceanic material making OC2 were decoupled at greater depth (40–50 km) from the sinking slab and in lesser amounts than OC1. The peak burial depth range of 30–40 km for OC2 corresponds to the downdip end of most seismogenic zones, to the source of episodic tremor and slip (Dragert et al., 2001; Rogers and Dragert, 2003) and to depths infered for present-day (Singh et al., 2008) or past tectonic slicing (Monié and Agard, 2009). Decoupling at such depths may therefore tentatively be related to seismic events occurring at depths (for deeper evidence, see Angiboust et al., 2012a,b). Whether such decoupling occurs continuously during oceanic subduction or at time intervals is completely unknown. In absence of radiometric constraints, it is difficult to argue whether those oceanic units were exhumed early (i.e. during oceanic subduction) or not (after the beginning of continental subduction). Given the fact that OC2 represents only small amounts of high-pressure oceanic material and is deformed in a similar way to the underlying Orhaneli unit, we suggest that the (previously decoupled) OC2 material was returned due to the exhumation of the continental unit (Fig. 9). Return of the continental material was likely triggered by buoyancy forces and/or changes in mechanical coupling along the plate interface at depths of ~75–80 km i.e. 22–25 kbar; Agard et al., 2009; Wada and Wang, 2009; Syracuse et al., 2010). In any case, it should be noted that almost all the oceanic crust (and lithosphere) was subducted and was never returned.

6.3. Comparison with the Oman case study and geodynamic implications

Obduction in Western Anatolia is compared in the following to the classic obduction of the Semail ophiolite (Boudier et al., 1988; Coleman, 1981; Ricou, 1971). A schematic palaeogeographic reconstruction of the northern Anatolide–Tauride margin, based on available data and on the fieldwork presented here, is shown at 90 Ma (Fig. 10). The two settings are characterized, at the onset of continental subduction

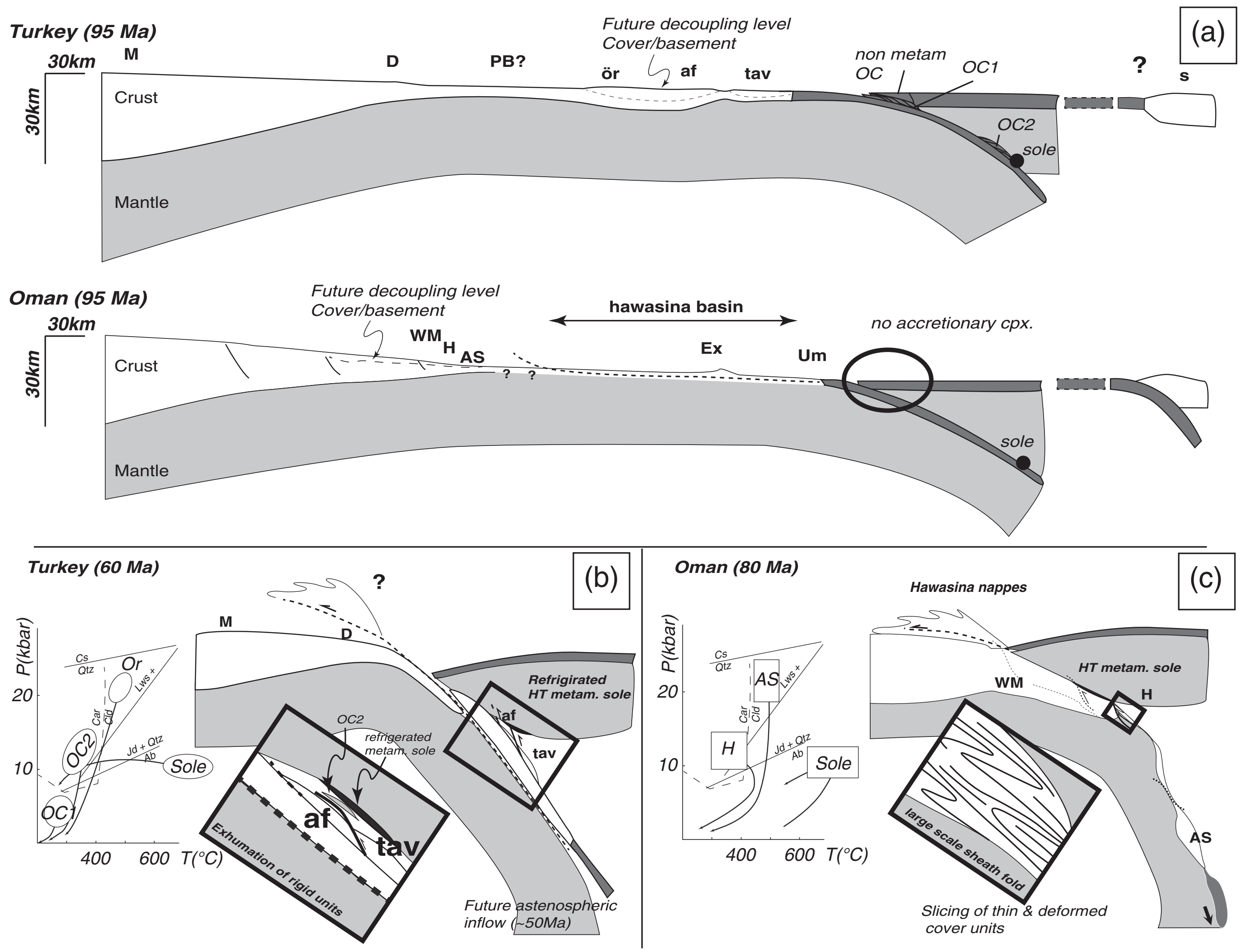

Fig. 10. (a) Supposed palaeogeographic setting for Western Anatolia and Oman after the initiation of an intra-oceanic subduction. Similarities and differences explained in text (Section 6.3); (b) Collision time sketches for Western Anatolia and associated PT conditions (c) Collision time sketches for Oman and associated PT conditions. Abbreviation are the following, M: Menderes; D: Dilek Nappes (Cycladic Blueschsits); PB: Pindos Basin; ör: Ören; af: Afyon; tav: Tavşanlı; S: Sakarya; WM: Wadi Mayh; H: Hulw; AS: As Sifah; Ex: Exotiques; Um: Umar.

(following initiation of intra-oceanic subduction), by a stretched Gondwana-derived continental margin of comparable dimensions.

Metamorphic amphibolitic soles in Oman and Turkey give both similar PT conditions (8–12/750–850 °C and 8–10 kbar/700–800 °C; Okay et al., 1998; Searle and Cox, 2002) and age constraints for intra-oceanic subduction initiation (*ca.* 100–95 Ma; Hacker, 1994; Hacker and Mosenfelder, 1996; Önen and Hall, 1993). Similar peak PT conditions too were reached in the Orhaneli and in the Saih Hatat/As Sifah eclogitic units (22 kbar–480 °C and 20 kbar–500 °C respectively; Warren and Waters, 2006; this study), coevally, at *ca.* 80 Ma (Hacker et al., 1996; Searle and Cox, 1999; Searle et al., 2004; Sherlock and Kelley, 2002; Sherlock et al., 1999). Both units correspond to the distal cover of the continental margin and show stretching lineations, observed for both exhumation (Boudier et al., 1988; Jolivet et al., 1998; Michard et al., 1985; Yamato et al., 2007) or peak burial conditions (Gautier, 1984; this study), that are sub-parallel to the direction of transport of the ophiolite. A pressure gap separates these units from units on top, which equilibrated at of 10–15 kbar and 300–400 °C (respectively the Ruwi, Mayh and Hulw continental units in Oman: Agard et al., 2010; Yamato et al., 2007); OC1 and OC2 in Western Anatolia: this study).

Despite striking similarities, several important differences can be pointed out:

(1) The high-pressure blueschist-facies overprint of the metamorphic sole found in Turkey is absent in Oman. As discussed above, this corresponds in Turkey to a rapid change in thermal regime (~5 My; see Section 6.1), which is on the lower bound of what was proposed for the amphibolite- to blueschist-facies rocks of the Catalina Schist in the Franciscan belt (Grove et al., 2008). Existence of this systematic HP–LT overprint in the Tavşanlı zone can be tentatively related either to (a) rapid cooling due to the stacking at similar depths (~10 kbar) of cold oceanic material (OC2) in the subduction zone and/or to (b) the an earlier exhumation of metamorphic soles in Oman compared to Turkey. Although the OC1 and OC2 oceanic units are systematically welded to the metamorphic sole, we note that (i) OC1 equilibrated to lower pressures than the metamorphic sole, (ii) OC2 shows comparable PT conditions yet no direct contact to the sole and that (iii) no amphibolite slice was found in any of the accretionary complexes. These observations indicate that the tectonic contact of the metamorphic sole onto OC1 cannot represent

the early, initial contact between the sole and accreted oceanic material and that, in order to support hypothesis (a), juxtaposed cold oceanic material (such as OC2) needed in sufficient amounts to refrigerate the metamorphic sole must have disappeared since.

Incidentally, we stress that emplacement mechanisms allowing metamorphic soles to become tectonically and rheological welded to the base of the ophiolite mantle, and the mismatch in P between peak burial (i.e., 30 km) and preserved ophiolite thickness (~10–15 km) both remain enigmatic.

(2) Accreted oceanic HP–LT units (OC1 and OC2) sandwiched between the continental margin and the unmetamorphosed obducted ophiolite are present in the Tavşanlı zone, whereas the distal, continental to oceanic Hawasina nappes are unmetamorphosed in Oman (Bechennec et al., 1990; de Wever et al., 1988). This could be explained in Oman by the existence of (i) a shallower decoupling level, at the base of the Hawasina basin, located mainly above the crustal basaltic layer and (ii) subduction of all oceanic material. In Western Anatolia, the Lycian nappes represent the tectonic equivalent of the Hawasina nappes and could tentatively root north of Menderes. However, evidence of sedimentation up to the Palaeocene in the Lycian nappes (coincident with HP–LT metamorphism of the Afyon zone and followed by Eocene granodioritic intrusions in Tavşanlı HP–LT units), suggests diachronic deposition in several domains (including the Ören unit and the northern edge of Menderes massif; Fig. 10; de Graciansky, 1972; Robertson, 1998; Collins and Robertson, 1999; Pourteau, 2011) and that they can only partly be equivalent to the Oman Hawasina nappes.

(3) HP–LT continental units are largely undeformed in Turkey and behaved as a thick and rigid crustal fragment. By contrast, HP–LT continental units in Oman consist of highly deformed, thin slices of cover material (Agard et al., 2010; Searle and Alsop, 2007; Searle et al., 2004). This observation points to a more efficient decoupling along the plate interface during continental subduction in Turkey than in Oman. We note that a somewhat deeper decoupling crustal layer is also required in Turkey to explain the presence of these thick and fairly undeformed high-pressure units.

All the above differences provide constraints on the early dynamics of subduction inception, oceanic subduction and burial/exhumation of the leading edge of continental margin (all of which predate the mild Eocene collision in Turkey, which has not yet affected Oman). They suggest the existence of contrasts in mechanical coupling and/or thermal regime between Turkey and Oman and allow one to propose that:

1- the rigid exhumation of Tavşanlı continental units and related mechanical decoupling is permitted by the presence of oceanic units, which acted like a lubricant between the continent and the mantle wedge and were partially entrained, as attested by OC2, during continental exhumation;
2- mechanical coupling evolved through time in the Tavşanlı subduction zone from strong, as oceanic units were underplated and the metamorphic sole was cooled (by contrast to Oman) to weak, thereby promoting continental burial and exhumation with only minor deformation;
3- the accretion of oceanic material is controlled by the depth of the initial décollement, which was deeper in Turkey than in Oman.

Several major unknowns remain on Mesozoic geodynamics of Western Anatolia. One is the uncertain existence of a subduction zone below Eurasia during Cretaceous times, as documented in Central Anatolia or on the Oman transect (Fig. 10; Agard et al., 2007; Okay et al., 2001; Okay et al. 2006, Lefebvre et al., 2013). The second one is the enigmatic, long-lived continental subduction and successive accretion in Western Anatolia of the Tavşanlı, Afyon, and (partially) Menderes domains over 30 My (from ~85–80 to 50–35 Ma). The absence of thorough collision across the İzmir–Ankara suture zone (contrary to Tibet or Iran; Agard et al., 2011; Hatzfeld and Molnar, 2010) may relate to the lack of subduction under Eurasia to the north and/or to its migration southwards as in the Cyclades (Jolivet and Brun, 2008), possibly due to mantle delamination (Van Hinsbergen et al., 2010). We suggest that this could also explain why convergence was taken up by continental subduction for so long (as long as in Norway, but without any UHP rocks returned; Labrousse et al., 2004).

7. Conclusions

The tectono-metamorphic evolution of extensive exposures of HP–LT cover units in the Tavşanlı zone (Western Anatolia), both oceanic and continental, provides critical information on exhumation mechanisms and regional-scale geodynamics.

The Tavşanlı zone shows consistent deformation patterns on a regional scale and minor deformation in exhumed continental rocks. PT conditions are homogeneous in the various units, with pressure gaps in between. From bottom to top, these comprise the continental Orhaneli unit (22 kbar, 480 °C), oceanic complex 2 (OC2; 11–13 kbar, 250–350 °C), oceanic complex 1 (OC1; 4–8 kbar, 250–300 °C), and the metamorphic sole (8–10 kbar, with temperatures evolving from 700–800 °C to ~300 °C). The absence of a retrograde overprint over such a large area suggests the rapid and/or cold exhumation of coherent units after the HP–LT stage.

Comparison with the Semail obduction setting allows highlighting similarities (i.e., overall palaeogeography, PT estimates for continental high-pressure domains, time elapsed between obduction and continental subduction, general orientation of stretching lineations with respect to subduction orientation) and some major differences. These include the presence, in Western Anatolia, of oceanic HP–LT material accreted between the plates and of a systematic HP–LT overprint on the amphibolitic metamorphic sole indicative of rapid cooling of the subduction zone (after subduction initiation) in <5 My.

The presence of the two metamorphic oceanic units in the Tavşanlı zone (OC1 and 2), the latter containing the first reported occurrences of Fe–Mg carpholite, allows constraining accretionary processes along the plate interface. These oceanic units were decoupled from the slab a different depths (~15–20 km, ~40 km). No evidence of a mélange structure or continuous corner-flow exhumation exist for these oceanic units. We suggest that the exhumation of these (previously accreted) units results from the fairly rigid and buoyant exhumation of the Orhaneli continental unit.

We finally suggest that mechanical coupling along the plate interface evolved from strong to weak during oceanic subduction and permitted the later subduction of the thinned continental margin at relatively great depths (70–80 km) and the rigid exhumation of the continental Orhaneli unit (and then, similarly, of the Afyon and Menderes units).

Acknowledgements

All authors thanks PHC Bosphorus joint project. (26289UD). Detailed reviews by D.J.J Van Hinsbergen and an anonymous reviewer were much appreciated and helped improve the manuscript. A. Plunder thanks A. Pourteau for helpful and stimulating discussions about Western Anatolia and Fe-Mg Carpholite during the preparation of this work. M. Fialin and the CAMPARIS analytical platform are thanked for access to EPMA facilities and assistance. D. Deldicque is thanked for access to SEM and Raman facilities at ENS.

References

Agard, P., Vitale-Brovarone, A., 2013. Thermal regime of continental subduction: the record from exhumed HP–LT terranes (New Caledonia, Oman, Corsica). Tectonophysics 601, 206–215.

Agard, P., Monié, P., Jolivet, L., Goffe, B., 2002. Exhumation of the Schistes Lustrés complex: in situ laser probe Exhumation of the Schistes Lustre Ar / Ar constraints and implications for the Western Alps. Journal of Metamorphic Geology 20, 599–618.

Agard, P., Jolivet, L., Vrielynck, B., Burov, E., Monié, P., 2007. Plate acceleration: the obduction trigger? Earth and Planetary Science Letters 258, 428–441.

Agard, P., Yamato, P., Jolivet, L., Burov, E., 2009. Exhumation of oceanic blueschists and eclogites in subduction zones: timing and mechanisms. Earth-Science Reviews 92, 53–79.

Agard, P., Searle, M.P., Alsop, G.I., Dubacq, B., 2010. Crustal stacking and expulsion tectonics during continental subduction: P–T deformation constraints from Oman. Tectonics 29, TC5018.

Agard, P., Omrani, J., Jolivet, L., Whitechurch, H., Vrielynck, B., Spakman, W., Monié, P., Meyer, B., Wortel, R., 2011. Zagros orogeny: a subduction-dominated process. Geological Magazine 148, 692–725.

Altunkaynak, S., 2007. Collision-driven slab breakoff magmatism in northwestern Anatolia, Turkey. Journal of Geology 63–82.

Angiboust, S., Agard, P., 2010. Initial water budget: the key to detaching large volumes of eclogitized oceanic crust along the subduction channel? Lithos 120, 453–474.

Angiboust, S., Agard, P., Yamato, P., Raimbourg, H., 2012a. Eclogite breccias in a subducted ophiolite: a record of intermediate-depth earthquakes? Geology 40, 707–710.

Angiboust, S., Langdon, R., Agard, P., Waters, D., Chopin, C., 2012b. Eclogitization of the Monviso ophiolite (W. Alps) and implications on subduction dynamics. Journal of Metamorphic Geology 30, 37–61.

Angiboust, S., Agard, P., De Hoog, J.C.M., Omrani, J., Plunder, A., 2013. Insights on deep, accretionary subduction processes from the Sistan ophiolitic "mélange" (Eastern Iran). Lithos 156–159, 139–158.

Bailey, E.H., 1981. Geologic map of Muscat-Ibra area, Sultanate of Oman, pocket map. Journal of Geophysical Research B4.

Baş, H., 1986. Tertiary geology of the Domaniç–Tavşanlı–Kütahya–Gediz region. Jeoloji Mühendisligi 17, 11–18.

Bechennec, F., Le Metour, J., Rabu, D., Bourdillon-de Grissac, C., de Wever, P., Beurrier, M., Villey, M., 1990. Structural evolution of a fragment of the south-Tethyan passive continental margin. Geological Society, London, Special Publications 49, 213–223.

Beyssac, O., Goffe, B., Chopin, C., Rouzaud, J.-N., 2002. Raman spectra of carbonaceous material in metasediments: a new geothermometer. Journal of Metamorphic Geology 20, 859–871.

Beyssac, O., Goffé, B., Petitet, J.-P., Froigneux, E., Moreau, M., Rouzaud, J.-N., 2003. On the characterization of disordered and heterogeneous carbonaceous materials by Raman spectroscopy. Spectrochimica Acta Part A: Molecular and Biomolecular Spectroscopy 59, 2267–2276.

Black, P.M., Maurizot, P., Ghent, E.D., Stout, M.Z., 1993. Mg–Fe carpholites from aluminous schists in the Diahot region and implications for preservation of high-pressure/low-temperature schists, northern New Caledonia. Journal of Metamorphic Geology 11, 455–460.

Boudier, F., Ceuleneer, G., Nicolas, A., 1988. Shear zones, thrusts and related magmatism in the Oman ophiolite: initiation of thrusting on an oceanic ridge. Tectonophysics 151, 275–296.

Bragin, N.Y.U., Tekin, U.K., 1996. Age of radiolarian-chert blocks from the Senonian Ophiolitic Melange (Ankara, Turkey). The Island Arc 5, 114–122.

Candan, O., Çetinkaplan, M., Oberhänsli, R., Rimmelé, G., Akal, C., 2005. Alpine high-P/low-T metamorphism of the Afyon Zone and implications for the metamorphic evolution of Western Anatolia, Turkey. Lithos 84, 102–124.

Çelik, Ö.F., Delaloye, M., Feraud, G., 2006. Precise 40 Ar–39 Ar ages from the metamorphic sole rocks of the Tauride Belt Ophiolites, southern Turkey: implications for the rapid cooling history. Geological Magazine 143, 213.

Çelik, Ö.F., Marzoli, A., Marschik, R., Chiaradia, M., Neubauer, F., Öz, İ., 2011. Early–Middle Jurassic intra-oceanic subduction in the İzmir–Ankara–Erzincan Ocean, Northern Turkey. Tectonophysics 509, 120–134.

Çetinkaplan, M., Candan, O., Oberhänsli, R., Bousquet, R., 2008. Pressure–temperature evolution of lawsonite eclogite in Sivrihisar; Tavşanlı Zone–Turkey. Lithos 104, 12–32.

Chemenda, A.I., Mattauer, M., Bokun, A.N., 1996. Continental subduction and a mechanicsm for exhumation of high-pressure metamorphic rocks: new modelling and field data from Oman. Earth and Planetary Science Letters 43, 173–182.

Chopin, C., Henry, C., Michard, A., 1991. Geology and petrology of the coesite-bearing terrain, Dora Maira massif, Western Alps. European Journal of Mineralogy 3, 263–291.

Cloos, M., 1982. Flow melanges: numerical modeling and geologic constraints on their origin int the Franciscan subduction complex, California. Geological Society of America Bulletin 93, 330–345.

Cloos, M., Shreve, R.L., 1988a. Subduction-channel model of prism accretion, melange formation, sediment subduction, and subduction erosion at convergent plate margins: 2. Implications and discussion. Pure and Applied Geophysics PAGEOPH 128, 501–545.

Cloos, M., Shreve, R.L., 1988b. Subduction-channel model of prism accretion, melange formation, sediment subduction, and subduction erosion at convergent plate margins: 1. Background and description. Pure and Applied Geophysics 128, 455–500.

Coggon, R., Holland, T.J.B., 2002. Mixing properties of phengitic micas and revised garnet–phengite thermobarometers. Journal of Metamorphic Geology 20, 683–696.

Cogulu, E., 1967. Etude petrographique de la region de Mihalliccik (Turquie). Schweizerische Mineralogische und Petrographische Mitteilungen 47, 683–824.

Coleman, R.G., 1981. Tectonic setting for ophiolite obduction in Oman. Journal of Geophysical Research 86, 2497–2508.

Collins, A.S., Robertson, A.H.F., 1997. Lycian melange, southwestern Turkey: an emplaced Late Cretaceous accretionary complex. Geology 3, 255–258.

Collins, A.S., Robertson, A.H.F., 1999. Evolution of the Lycian Allochthon, western Turkey, as a north-facing Late Palaeozoic to Mesozoic rift and passive continental margin. Geological Journal 34, 107–138.

Connolly, J.A.D., 2005. Computation of phase equilibria by linear programming: a tool for geodynamic modeling and its application to subduction zone decarbonation. Earth and Planetary Science Letters 236, 524–541.

Connolly, J.A.D., 2009. The geodynamic equation of state: what and how. Geochemistry, Geophysics, Geosystems 10, Q10014. http://dx.doi.org/10.1029/2009GC002540.

Connolly, J.A.D., Kerrick, D.M., 1987. An algorithm and computer program for calculating composition phase diagrams. Calphad 11, 1–55.

Davis, P.B., Whitney, D.L., 2006. Petrogenesis of lawsonite and epidote eclogite and blueschist, Sivrihisar Massif, Turkey. Journal of Metamorphic Geology 24, 823–849.

Davis, P.B., Whitney, D.L., 2008. Petrogenesis and structural petrology of high-pressure metabasalt pods, Sivrihisar, Turkey. Contributions to Mineralogy and Petrology 156, 217–241.

de Graciansky, P.-C., 1972. Recherches Géologiques dans le Taurus Lycien Occidental. PhD thesis. Université de Paris-Sud, Orsay.

De Wever, P., Bourdillon-de Grissac, C., Bechennec, F., 1988. Permian age from radiolarites of the Hawasina nappes Oman mountains. Geology 16, 912–914.

Diener, J.F.A., Powell, R., 2012. Revised activity-composition models for clinopyroxene and amphibole. Journal of Metamorphic Geology 30, 131–142.

Dilek, Y., Altunkaynak, S., 2009. Geochemical and temporal evolution of Cenozoic magmatism in western Turkey: mantle response to collision, slab break-off, and lithospheric tearing in an orogenic belt. Geological Society, London, Special Publications 311, 213–233.

Dilek, Y., Whitney, D.L., 1997. Counterclockwise P–T–t trajectory from the metamorphic sole of a Neo-Tethyan ophiolite (Turkey). Tectonophysics 280, 295–310.

Dilek, Y., Thy, P., Hacker, B., Grundvig, S., 1999. Structure and petrology of Tauride ophiolites and mafic dike intrusions (Turkey): implications for the Neotethyan ocean. Geological Society of America Bulletin 111, 1192–1216.

Dragert, G., Wang, K., James, T.S., 2001. A silent slip event on the deeper Cascadia subduction interface. Science 292, 1525–1528.

Droop, G.T.R., Karakaya, M., Eren, Y., Karakaya, N., 2005. Metamorphic evolution of blueschists of the Altınekin Complex, Konya area, south central Turkey. Geological Journal 40, 127–153.

Ernst, W.G., 1973. Interpretative synthesis of the metamorphism in the Alps. Bulletin of the Geological Society of America 84, 2053–2078.

Evans, B.W., 1990. Phase relations of epidote-blueschists. Lithos 25, 3–23.

Festa, A., Dilek, Y., Pini, G.A., Codegone, G., Ogata, K., 2012. Mechanisms and processes of stratal disruption and mixing in the development of mélanges and broken formations: redefining and classifying mélanges. Tectonophysics 568–569, 7–24.

Gautier, Y., 1984. Deformation et métamorphismes associés à la suture Thethysienne en Anatolie centrale (Région de Sivrihisar, Turquie). PhD thesis. Université de Paris-Sud, Orsay.

Gessner, K., Collins, A.S., Ring, U., GÜngÖr, T., 2004. Structural and thermal history of poly-orogenic basement: U–Pb geochronology of granitoid rocks in the southern Menderes Massif, Western Turkey. Journal of the Geological Society 161, 93–101.

Gessner, K., Gallardo, L.A., Markwitz, V., Ring, U., Thomson, S.N., 2013. What caused the denudation of the Menderes Massif: review of crustal evolution, lithosphere structure, and dynamic topography in southwest Turkey. Gondwana Research 24, 243–274.

Goffé, B., Michard, A., Kienast, J.R., Le Mer, O., 1988. A case of abduction-related metamorphism in upper crustal nappes, Arabian continental margin, Oman: P–T paths and kinematic interpretation. Tectonophysics 151, 363–386.

Göncüoglu, M.C., Yalınız, M.K., Tekin, U.K., 2006. Geochemistry, tectono-magmatic discrimination and radiolarian ages of basic extrusives within the Izmir–Ankara suture belt (NW Turkey): time constraints for the Neotethyan evolution. Ofioliti 31, 25–38.

Göncüoglu, M.C., Sayit, K., Tekin, U.K., 2010. Oceanization of the northern Neotethys: geochemical evidence from ophiolitic melange basalts within the İzmir–Ankara suture belt, NW Turkey. Lithos 116, 175–187.

Grove, M., Kimbrough, D.L., Zou, H., 2008. The Catalina Schist: evidence for Mid-Cretaceous subduction erosion of Southwestern North America. Geological Society of America Special Papers 436, 335–361.

Gutnic, M., Monod, O., Poisson, A., Dumont, J.-F., 1979. Géologie des Taurides occidentales (Turquie). Mémoires de de la Société géologique de France 137, 1–112.

Hacker, B.R., 1994. Rapid emplacement of young oceanic lithosphere: argon geochronology of the Oman ophiolite. Science 265, 1563–1565.

Hacker, B.R., Mosenfelder, J.L., 1996. Metamorphism and deformation along the emplacement thrust of the Samail ophiolite, Oman. Earth and Planetary Science Letters 144, 435–451.

Hacker, B.R., Mosenfelder, J.L., Gnos, E., 1996. Rapid emplacement of the Oman ophiolite: thermal and geochronogic constraints. Tectonics 15, 1230–1247.

Harris, N.B.W., Kelley, S., Okay, A.I., 1994. Post-collision magmatism and tectonics in northwest Anatolia. Contributions to Mineralogy and Petrology 117, 241–252.

Hatzfeld, D., Molnar, P., 2010. Comparisons of the kinematics and deep structures of the Zagros and Himalaya and of the Iranian and Tibetan plateaus. Reviews of Geophysics 48, 1–48.

Holland, T.J.B., Powell, R., 1998. An internally consistent thermodynamic data set for phases of petrological interest. Journal of Metamorphic Geology 16, 309–343.

Holland, T.J.B., Baker, J., Powell, R., 1998. Mixing properties and activity–composition relationships of chlorites in the system MgO–FeO–Al2O3–SiO2–H2O. European Journal of Mineralogy 10, 395–406.

Jolivet, L., Brun, J.-P., 2008. Cenozoic geodynamic evolution of the Aegean. International Journal of Earth Sciences 99, 109–138.

Jolivet, L., Goffe, B., Bousquet, R., Oberhänsli, R., Michard, A., 1998. Detachments in high-pressure mountain belts, Tethyan examples. Earth and Planetary Science Letters 160, 31–47.

Jolivet, L., Faccenna, C., Goffé, B., Burov, E., Agard, P., Goffe, B., 2003. Subduction tectonics and exhumation of high-pressure metamorphic rocks in the Mediterranean orogens. American Journal of Science 303, 353–409.

Jolivet, L., Faccenna, C., Huet, B., Labrousse, L., Le Pourhiet, L., Lacombe, O., Lecomte, E., Burov, E., Denèle, Y., Brun, J.-P., Philippon, M., Paul, A., Salaün, G., Karabulut, H., Piromallo, C., Monié, P., Gueydan, F., Okay, A.I., Oberhänsli, R., Pourteau, A., Augier, R., Gadenne, L., Driussi, O., 2013. Aegean tectonics: strain localisation, slab tearing and trench retreat. Tectonophysics 597–598, 1–33.

Kaya, O., 1972. Outlines of the ophiolite question in the Tavsanli region (in Turkish). Bulletin of the Geological Society of Turkey 15, 26–108.

Kaya, O., Sadedd, W., Altiner, D., Meriç, E., Tansel, I., Vural, A., 1995. Stratigraphic and structural setting of the anchimetamorphic rocks to the south of Tavşanlı (Kütahya, western Turkey): relation to the Izmir–Ankara zone. Mineral research exploration bulletin 117, 5–16.

Kaya, O., Kozur, H., Sadeddin, W., Helvaci, H., 2001. Late Norian age for a metacarbonate unit in NW Anatolia, Turkey. Geobios 34, 527–532.

Khain, V.E., 1975. Structure and main stages in the tectonomagmatic development of the Caucasus: an attempt at geodynamic interpretation. American Journal of Science 275, 113–156.

Kienast, J.R., 1983. Le métamorphisme de haute pression et basse température (éclogite et schistes bleus): donnes nouvelles sur la pétrologie des roches de la croûte océanique subductée et des sédiments associés. PhD thesis. Université Pierre et Marie Curie, Paris.

Kimura, G., 1994. The latest Cretaceous–early Paleogene rapid growth of accretionary complex and exhumation of high pressure series metamorphic rocks in northwestern Pacific margin. Journal of Geophysical Research 99, 22147–22164.

Kopp, C., Fruehn, J., Flueh, E.R., Reichert, C., Kukowski, N., Bialas, J., 2000. Structure of the Makran subduction zone from wide-angle and reflection seismic data. Tectonophysics 329, 171–191.

Kretz, R., 1983. Symbols for rock-forming minerals. American Mineralogist 68, 277–279.

Kusky, T.M., Bradley, D.C., Haeussler, P., 1997. Progressive deformation of the Chugach accretionary complex, Alaska, during a paleogene ridge-trench encounter. Journal of Structural Geology 19, 139–157.

Labrousse, L., Jolivet, L., Andersen, T.B., Agard, P., Hébert, R., Maluski, H., Schärer, U., 2004. Pressure–temperature–time deformation history of the exhumation of ultra-high pressure rocks in the Western Gneiss Region, Norway. Geological Society of America Special Papers 380, 155–183.

Leake, B.E., Woolley, A.R., Arps, C.E.S., Birch, W., Gilbert, C., Grice, J., Hawthorne, F.C., Kato, A., Kisch, H.J., Krivovichev, V.G., Linthout, K., Laird, J., Mandarino, J.A., Maresch, W.V., Nickel, E., Schumacher, J.C., Smith, D., Stephenson, N., Ungarette, L., Whittaker, E., Youzhi, G., 1997. Nomenclature of amphiboles: report of the subcommittee on amphiboles of the international mineralogical association, commission on new minerals and mineral names. The Canadian Mineralogist 35, 219–246.

Lefebvre, C., Meijers, M.J.M., Kaymakci, N., Peynircioğlu, A., Langereis, C.G., van Hinsbergen, D.J.J., 2013. Reconstructing the geometry of central Anatolia during the late Cretaceous: large-scale Cenozoic rotations and deformation between the Pontides and Taurides. Earth and Planetary Science Letters 366, 83–98.

Lisenbee, A., 1972. Structural setting of the Orhaneli ultramafic massif near Bursa, Northwestern Turkey. PhD thesis. Pennsylvania State University, USA.

Lünel, T., 1967. Geology of Sübren, Karacaalan–Yukari Caglayan area. Eskişehir county, Turkey.

Manav, H., Gültekin, A.H., Uz, B., 2004. Geochemical evidence for the tectonic setting of the Harmancik ophiolites, NW Turkey. Journal of Asian Earth Sciences 24, 1–9.

Marschall, H.R., Schumacher, J.C., 2012. Arc magmas sourced from mélange diapirs in subduction zones. Nature Geoscience 5, 862–867.

Massonne, H.-J., Willner, A.P., 2008. Phase relations and dehydration behaviour of psammopelite and mid-ocean ridge basalt at very-low-grade to low-grade metamorphic conditions. European Journal of Mineralogy 20, 867–879.

Meijers, M.J.M., Langereis, C.G., van Hinsbergen, D.J.J., Kaymakcı, N., Stephenson, R.A., Altıner, D., 2010. Jurassic–Cretaceous low paleolatitudes from the circum-Black Sea region (Crimea and Pontides) due to True Polar Wander. Earth and Planetary Science Letters 296, 210–226.

Michard, A., Bouchez, J.L., Misseri, M., 1981. Les nappes metamorphiques de Mascate, nouvel élément infraophiolitique en Oman. Terra Cognita 1, 19.

Michard, A., Juteau, T., Whitechurch, H., 1985. L'obduction: revue des modèles et confrontation au cas de l'Oman. Bulletin de la Société Géologique de France 2, 189–198.

Moix, P., Beccaletto, L., Kozur, H.W., Hochard, C., Rosselet, F., Stampfli, G.M., 2008. A new classification of the Turkish terranes and sutures and its implication for the paleotectonic history of the region. Tectonophysics 451, 7–39.

Monié, P., Agard, P., 2009. Coeval blueschist exhumation along thousands of kilometers: implications for subduction channel processes. Geochemistry, Geophysics, Geosystems 10, Q07002. http://dx.doi.org/10.1029/2009GC002428.

Monod, O., Andrieux, J., Gautier, Y., Kienast, J.R., 1991. Pontides–Taurides relationship in the region of Eskisehir (NW Turkey). Bulletin of the technical university of Istanbul 44, 257–278.

MTA, 2002. Geological map of Turkey, scale 1:500,000. Mineral Research and Exploration Institute of Turkey, Izmir.

Okay, A.I., 1978. Sodic pyroxenes from metabasite in the eastern Mediterranean. Contributions to Mineralogy and Petrology 1, 7–11.

Okay, A.I., 1980a. Lawsonite zone blueschists and a sodic amphibole producing reaction in the Tavşanlı Region, Northwest Turkey. Contributions to Mineralogy and Petrology 72, 243–255.

Okay, A.I., 1980b. Mineralogy, petrology and phase relations of Glaucophane–Lawsonite blueschists from the Tavşanlı region, northwest Turkey. Contributions to Mineralogy and Petrology 72, 243–255.

Okay, A.I., 1982. Incipient blueschist metamorphism and metasomatism in the Tavşanlı Region, Northwest Turkey. Contributions to Mineralogy and Petrology 79, 361–367.

Okay, A.I., 1986. High-pressure/low-temperature rocks of Turkey. In: Evans, B.W., Brown, E.H. (Eds.), Blueschists and Eclogites. Geological Society of America Memoir, pp. 333–347.

Okay, A.I., 2002. Jadeite–chloritoid–glaucophane–lawsonite blueschists in north-west Turkey: unusually high P/T ratios in continental crust. Journal of Metamorphic Geology 20, 757–768.

Okay, A.I., Kelley, S., 1994. Tectonic setting, petrology and geochronology of jadeite + glaucophane and chloritoid + glaucophane schsits from north-west Turkey. Journal of Metamorphic Geology 12, 455–466.

Okay, A.I., Satır, M., 2006. Geochronology of Eocene plutonism and metamorphism in northest Turkey: evidence for a possible magmatic arc. Geodinamica Acta 5, 251–266.

Okay, A.I., Tüysüz, O., 1999. Tethyan sutures of northern Turkey. Geological Society, London, Special Publications 156, 475–515.

Okay, A.I., Whitney, D.L., 2010. Blueschsits, eclogites, ophiolite and suture zones in Northwest Turkey: a review and a field excursion guide. Ofioliti 35, 131–172.

Okay, A.I., Harris, N.B.W., Kelley, S., 1998. Exhumation of blueschists along a Tethyan suture in northwest Turkey. Tectonophysics 285, 275–299.

Okay, A.I., Tansel, I., Tüysüz, O., 2001. Obduction, subduction and collision as reflected in the Upper Cretaceous–Lower Eocene sedimentary record of western Turkey. Geological Magazine 138, 117–142.

Okay, A.I., Tüysüz, O., Satır, M., Özkan-Altıner, S., Altıner, D., Sherlock, S., Eren, R.H., 2006. Cretaceous and Triassic subduction-accretion, high-pressure-low-temperature metamorphism, and continental growth in the Central Pontides, Turkey. Geological Society of America Bulletin 118, 1247–1269.

Okay, A.I., Satır, M., Shang, C.K., 2008. Ordovician metagranitoid from the Anatolide–Tauride Block, northwest Turkey: geodynamic implications. Terra Nova 20, 280–288.

Okay, A.I., İşintek, İ., Altıner, D., Özkan-Altıner, S., Okay, N., 2012. An olistostrome–mélange belt formed along a suture: Bornova Flysch zone, western Turkey. Tectonophysics 568–569, 282–295.

Önen, P., 2003. Neotethyan ophiolitic rocks of the Anatolides of NW Turkey and comparison with Tauride ophiolites. Geological Society, London, Special Publications 160, 947–962.

Önen, A.P., Hall, R., 1993. Ophiolites and related metamorphic rocks from the Kutahya region, north-west Turkey. Geological Journal 28, 399–412.

Önen, P., Hall, R., 2000. Sub-ophiolite metamorphic rocks from NW Anatolia, Turkey. Journal of Metamorphic Geology 18, 483–495.

Özbey, Z., Ustaömer, T., Robertson, A.H.F., Ustaömer, P.A., Dixon, J., 2010. Evidence for the tectonic development and subduction-exhumation of a Palaeozoic–Mesozoic continental margin in the westernmost Anatolides, W Turkey. Geophysical Research Abstract 12.

Özbey, Z., Ustaömer, T., Robertson, A.H.F., 2013a. Mesozoic magmatic and sedimentary development of the Tavsanli Zone (NW Turkey): implications for rifting, passive margin development and ocean crust emplacement. Geological Society, London, Special Publications 372.

Özbey, Z., Ustaömer, T., Robertson, A.H.F., Ustaömer, P.A., 2013b. Tectonic significance of Late Ordovician granitic magmatism and clastic sedimentation on the northern margin of Gondwana (Tavsanli Zone, NW Turkey). Journal of the Geological Society 170, 159–173.

Özgen-Erdem, N., Akyazı, M., Karabaşoğlu, A., 2007. Biostratigraphic interpretation and systematics of Alveolina assemblages from the Ilerdian–Cuisian limestones of Southern Eskişehir, Central Turkey. Journal of Asian Earth Sciences 29, 911–927.

Pamic, J., Tomljenovic, B., Balen, D., 2002. Geodynamic and petrogenetic evolution of Alpine ophiolites from the central and NW Dinarides: an overview. Lithos 65, 113–142.

Parlak, O., Delaloye, M., 1999. Precise $^{40}Ar/^{39}Ar$ ages from the metamorphic sole of the Mersin ophiolite (southern Turkey). Tectonophysics 301, 145–158.

Peacock, S., 1996. Thermal and petrologic structure of subduction zones. In: Bebout, Gray E., Scholl, D.W., Kirby, S.H., Platt, J.P. (Eds.), Subduction: Top to Bottom.

Platt, J.P., 1986. Dynamics of orogenic wedges and the uplift of high-pressure metamorphic rocks. Geological Society of America Bulletin 97, 1037–1053.

Platt, J., 1993. Exhumation of high-pressure metamorphic rocks: a review of concepts and processes. Terra Nova 5, 119–133.

Plunder, A., Agard, P., Dubacq, B., Chopin, C., Bellanger, M., 2012. How continuous and precise is the record of P–T paths? Insights from combined thermobarometry and thermodynamic modelling into subduction dynamics (Schistes Lustrés, W. Alps). Journal of Metamorphic Geology 30, 323–346.

Plunder, A., Agard, P., Chopin, C., Okay, A., 2013. Record of high-pressure overprint in metamorphic soles of the Tavşanlı zone, western Anatolia. Geophysical Research Abstract 15, 8465.

Pourteau, A., 2011. Closure of the Neotethys Ocean in Anatolia: structural, petrologic & geochronologic insights from low-grade high-pressure metasediments. Afyon Zone. Ph D Thesis, Potsdam University, Germany.

Pourteau, A., Candan, O., Oberhänsli, R., 2010. High-pressure metasediments in central Turkey: constraints on the Neotethyan closure history. Tectonics 29, TC5004.

Pourteau, A., Sudo, M., Candan, O., Lanari, P., Vidal, O., Oberhänsli, R., 2013. Neotethys closure history of Anatolia: insights from 40 Ar–39 Ar geochronology and P–T estimation in high-pressure metasedimentary rocks. Journal of Metamorphic Geology 31, 585–606.

Ricou, L.E., 1971. Le croissant ophiolitique péri-arabe, une ceinture de nappes mise en place au crétacé supérieur. Revue de Géographie Physique et de Géologie Dynamique 13, 327–350.

Rimmelé, G., Parra, T., Goffé, B., Oberhänsli, R., Jolivet, L., Cadan, O., 2004. Exhumation paths of high-pressure–low-temperature metamorphic rocks from the Lycian Nappes and the Menderes Massif (SW Turkey): a multi-equilibrium approach. Journal of Petrology 46, 641–669.
Robertson, A.H.F., 1998. Mesozoic—tertiary tectonic evolution of the easternmost mediterranean area: integration of marine and land evidence. Proceedings of the Ocean Drilling Program, Scientific Results 160, 723–782.
Robertson, A.H., 2002. Overview of the genesis and emplacement of Mesozoic ophiolites in the Eastern Mediterranean Tethyan region. Lithos 65, 1–67.
Rogers, G., Dragert, H., 2003. Episodic tremor and slip on the Cascadia subduction zone: the chatter of silent slip. Science 300, 1942–1943.
Sarıfakıoğlu, E., Özen, H., Winchester, J.A., 2009. Whole rock and mineral chemistry of ultramafic–mafic cumulates from the Orhaneli (Bursa) ophiolite, NW Anatolia. Turkish Journal of Earth Science 18, 55–83.
Sarıfakıoğlu, E., Özen, H., Çolakoğlu, A., Sayak, H., 2010. Petrology, mineral chemistry, and tectonomagmatic evolution of Late Cretaceous suprasubduction-zone ophiolites in the İzmir–Ankara–Erzincan suture zone, Turkey. International Geology Review 52, 187–222.
Schmid, S.M., Bernoulli, D., Fügenschuh, B., Matenco, L., Schefer, S., Schuster, R., Tischler, M., Ustaszewski, K., 2008. The Alpine–Carpathian–Dinaridic orogenic system: correlation and evolution of tectonic units. Swiss Journal of Geosciences 101, 139–183.
Searle, M.P., Alsop, G.I., 2007. Eye-to-eye with a mega-sheath fold: a case study from Wadi Mayh, northern Oman Mountains. Geology 35, 1043–1046.
Searle, M., Cox, J., 1999. Tectonic setting, origin, and obduction of the Oman ophiolite. Geological Society of America Bulletin 111, 104–122.
Searle, M.P., Cox, J., 2002. Subduction zone metamorphism during formation and emplacement of the Semail ophiolite in the Oman Mountains. Geological Magazine 139, 241–255.
Searle, M., Waters, D.J., Martin, H.N., Rex, D.C., 1994. Structure and metamorphism of blueschist–eclogite facies rocks from the north-eastern Oman mountains. Journal of the Geological Society of London 151.
Searle, M., Warren, C., Waters, D., Parrish, R., 2004. Structural evolution, metamorphism and restoration of the Arabian continental margin, Saih Hatat region, Oman Mountains. Journal of Structural Geology 26, 451–473.
Seaton, N.C.A., Whitney, D.L., Teyssier, C., Toraman, E., Heizler, M.T., 2009. Recrystallization of high-pressure marble (Sivrihisar, Turkey). Tectonophysics 479, 241–253.
Sengör, A.M.C., Yılmaz, Y., 1981. Tethyan evolution of Turkey: a plate tectonic approach. Tectonophysics 75, 181–241.
Servais, M., 1981. Données préliminaires sur la zone de suture médio-téthysienne dans la région d'Eskisehir (NW Anatolie). Comptes rendus de l'Académie des Sciences 293, 83–86.
Servais, M., 1982. Collision et suture téthysienne en Anatolie Centrale, étude structurale et métamorphique (HP-BT) de la zone nord Kütahya. PhD Thesis. Université Paris-Sud, Orsay.
Sherlock, S., Kelley, S., 2002. Excess argon evolution in HP–LT rocks: a UVLAMP study of phengite and K-free minerals, NW Turkey. Chemical Geology 182, 619–636.
Sherlock, S., Kelley, S., Inger, S., Harris, N., Okay, A.I., 1999. Ar–39 Ar and Rb–Sr geochronology of high-pressure metamorphism and exhumation history of the Tavsanli Zone, NW Turkey. Contributions to Mineralogy and Petrology 137, 46–58.
Shin, T.A., Catlos, E.J., Jacob, L., Black, K., 2013. Relationships between very high pressure subduction complex assemblages and intrusive granitoids in the Tavşanlı Zone, Sivrihisar Massif, central Anatolia. Tectonophysics 595–596, 183–197.
Singh, S.C., Carton, H., Tapponnier, P., Hananto, N.D., Chauhan, A.P.S., Hartoyo, D., Bayly, M., Moeljopranoto, S., Bunting, T., Christie, P., Lubis, H., Martin, J., 2008. Seismic evidence for broken oceanic crust in the 2004 Sumatra earthquake epicentral region. Nature Geoscience 1, 777–781.
Spray, J.G., 1984. Possible Causes and Consequences of Upper Mantle Decoupling and Ophiolite Displacement. Geological Society, London, Special Publications 13, 255–268.
Syracuse, E.M., van Keken, P.E., Abers, G.A., 2010. The global range of subduction zone thermal models. Physics of the Earth and Planetary Interiors 183, 73–90.
Tekin, U.K., Göncüoglu, M.C., 2007. Discovery of the oldest (Upper Ladinian to Middle Carnian) radiolarian assemblages from the Bornova Flysch Zone in western Turkey: implications for the evolution of the Neotethyan Izmir–Ankara Ocean. Ofioliti 32, 131–150.
Tekin, U.K., Göncüoglu, M., 2009. Late Middle Jurassic (Late Bathonian–early Callovian) radiolarian cherts from the Neotethyan Bornova flysch zone, Spil Mountains, Western Turkey. Stratigraphy and Geological Correlation 17, 298–308.
Tekin, U.K., Göncüoglu, M., Turhan, N., 2002. First evidence of Late Carnian radiolarians from the Izmir–Ankara suture complex, central Sakarya, Turkey: implications for the opening age of the Izmir–Ankara branch of Neo-Tethys. Geobios 35, 127–135.
Thomson, S.N., Ring, U., 2006. Thermochronologic evaluation of postcollision extension in the Anatolide orogen, western Turkey. Tectonics 25, TC3005. http://dx.doi.org/10.1029/2005TC001833.
Topuz, G., Okay, A.I., Altherr, R., Meyer, H.-P., Nasdala, L., 2006. Partial high-pressure aragonitization of micritic limestones in an accretionary complex, Tavşanlı Zone, NW Turkey. Journal of Metamorphic Geology 24, 603–613.
Topuz, G., Gocmengil, G., Rolland, Y., Celik, O.F., Zack, T., Schmitt, A.K., 2012. Jurassic accretionary complex and ophiolite from northeast Turkey: no evidence for the Cimmerian continental ribbon. Geology 41, 255–258.
Van der Kaaden, G., 1966. The signifiance and distribution of glaucophane rocks in Turkey. Bulletin. Mineral Research and Exploration Institute 67, 37–67.
Van Hinsbergen, D.J.J., Schmid, S.M., 2012. Map view restoration of Aegean–West Anatolian accretion and extension since the Eocene. Tectonics 31, TC5005.
Van Hinsbergen, D.J.J., Kaymakci, N., Spakman, W., Torsvik, T.H., 2010. Reconciling the geological history of western Turkey with plate circuits and mantle tomography. Earth and Planetary Science Letters 297, 674–686.
Van Keken, P.E., Hacker, B.R., Syracuse, E.M., Abers, G.A., 2011. Subduction factory: 4. Depth-dependent flux of H_2O from subducting slabs worldwide. Journal of Geophysical Research 116, B01401. http://dx.doi.org/10.1029/2010JB007922.
Vitale-Brovarone, A., Groppo, C., Hetényi, G., Compagnoni, R., Malavieille, J., 2011. Coexistence of lawsonite-bearing eclogite and blueschist: phase equilibria modelling of Alpine Corsica metabasalts and petrological evolution of subducting slabs. Journal of Metamorphic Geology 29, 583–600.
Wada, I., Wang, K., 2009. Common depth of slab-mantle decoupling: reconciling diversity and uniformity of subduction zones. Geochemistry, Geophysics, Geosystems 10, Q10009.
Wakabayashi, J., 1990. Counterclockwise P–T–t paths from amphibolites, Franciscan Complex, California: relics from the early stages of subduction zone metamorphism. Geological Journal 98, 657–680.
Wakabayashi, J., 2011. Mélanges of the Franciscan Complex, California: diverse structural settings, evidence for sedimentary mixing, and their connection to subduction processes. The Geological society of America Special paper 480, 117–141.
Wakabayashi, J., Dilek, Y., 2003. What constitute "emplacement" of an ophiolite?: mechanisms and relationship to subduction initiation and formation of metamorphic soles. Geological Society, London, Special Publications 218, 427–447.
Warren, C.J., Waters, D.J., 2006. Oxidized eclogites and garnet-blueschists from Oman: P–T path modelling in the NCFMASHO system. Journal of Metamorphic Geology 24, 783–802.
Wei, C.J., Clarke, G.L., 2011. Calculated phase equilibria for MORB compositions: a reappraisal of the metamorphic evolution of lawsonite eclogite. Journal of Metamorphic Geology 29, 939–952.
Whitney, D.L., Davis, P.B., 2006. Why is lawsonite eclogite so rare? Metamorphism and preservation of lawsonite eclogite, Sivrihisar, Turkey. Geology 34, 473–476.
Woodcock, N.H., Robertson, A.H.F., 1977. Origins of some ophiolite-related metamorphic rocks of the "Tethyan" belt. Geology 5, 373–376.
Yamato, P., Agard, P., Goffé, B., De Andrade, V., Vidal, O., Jolivet, L., 2007. New, high-precision P–T estimates for Oman blueschists: implications for obduction, nappe stacking and exhumation processes. Journal of Metamorphic Geology 25, 657–682.